AD 262 466

NOTICE: When government or other drawings, specifications or other data are used for any purpose other than in connection with a definitely related government procurement operation, the U. S. Government thereby incurs no responsibility, nor any obligation whatsoever; and the fact that the Government may have formulated, furnished, or in any way supplied the said drawings, specifications, or other data is not to be regarded by implication or otherwise as in any manner licensing the holder or any other person or corporation, or conveying any rights or permission to manufacture, use or sell any patented invention that may in any way be related thereto.

AEDC-TN-61-83

DESCRIPTION AND PRELIMINARY CALIBRATION OF A LOW-DENSITY, HYPERVELOCITY WIND TUNNEL

By

J. Leith Potter, Max Kinslow,
George D. Arney, Jr., and Allan B. Bailey
VKF, ARO, Inc.

August 1961

ARNOLD ENGINEERING DEVELOPMENT CENTER
AIR FORCE SYSTEMS COMMAND
USAF

AEDC-TN-61-83

DESCRIPTION AND PRELIMINARY CALIBRATION OF A LOW-DENSITY, HYPERVELOCITY WIND TUNNEL

By

J. Leith Potter, Max Kinslow,
George D. Arney, Jr., and Allan B. Bailey

VKF, ARO, Inc.

August 1961

ARO Project Nos. 306060 and 306970
AFSC Program Area 750A, Project No. 8950, Task 89602

Contract No. AF 40(600)-800 S/A 24(61-73)

ABSTRACT

A small, low-density, hypervelocity, continuous wind tunnel operating at total temperatures from 2000 to 4000 °K is described, and initial experiments designed to determine the characteristics of the flow are discussed. Effects of low Reynolds numbers on impact-pressure probes and static-pressure probes are shown. Preliminary work with a probe for measuring local mass-flow rate is outlined, and results are shown to be in agreement with impact and static pressure measurements. Axial and transverse surveys of flow in the nozzle are presented to illustrate the extent of boundary-layer growth and the useable core of flow. A diffuser is proved to be advantageous, even though very low Reynolds numbers are typical of the tunnel. A comparison of data on drag of spheres, including measurements from the new wind tunnel, is presented.

CONTENTS

ILLUSTRATIONS

NOMENCLATURE

A	Cross-sectional area or reference area
C_D	Drag coefficient
C_F	Force coefficient, either lift or drag
D	Reference diameter, usually maximum
d	Orifice or inside diameter
h	Height of manometer or gage fluid column
M	Mach number
$\dot{m}$	Mass-flow rate
p	Pressure
q	Dynamic pressure, $\rho U^2/2$
R	Gas constant
r	Body or nose radius
S	Molecular speed ratio
T	Temperature
t	Time
U	Velocity
V	Volume
X	Axial station in nozzle, zero at exit, positive downstream
x	Axial length along probe, zero at stagnation point
Y	Radial station in nozzle, zero on centerline, positive downward
Z	$Z = p/\rho RT$
γ	Ratio of specific heats
ϵ	ρ_∞/ρ_2
μ	Denotes microns or 0.001 mm
ν	Kinematic viscosity
ρ	Density
σ	Shock wave angle measured from free-stream direction

SUBSCRIPTS

a	Dimensions of probe orifice
c	Near inviscid, high Reynolds number condition
fm	Free-molecular flow condition
i	Probe or tube inside diameter
o	Stagnation conditions (total or reservoir). When used in combination with a prime - i. e., p_o', conditions at the stagnation point on a body are referred to.
p	Conditions at inlet to mass-flow probe
∞	Free-stream conditions
1	Local value of a quantity
2	Conditions immediately downstream of a normal shock wave
t	Conditions in tank surrounding tunnel nozzle and jet
v	Conditions inside mass-flow collecting tank
w	Body surface or wall condition
x	Based on the distance x

INTRODUCTION

The need for studying gas dynamic problems created by flight at extreme altitudes has led to consideration of experimental facilities capable of simulating the essential flow conditions. Some of the preliminary design considerations pertaining to a small, prototype facility for exploring problems in the simulation of flight at extreme altitudes by wind tunnel techniques are discussed. Following this, the tunnel is described, and results of several early calibration tests are presented.

The process leading to construction of the prototype facility described herein included study of the flight regimes of various types of vehicles to determine what characteristics should be possessed by the laboratory simulator. This approach may quickly lead to impossible goals if duplication of all free-flight conditions is considered, and rather drastic compromises often are imposed by practical considerations. Many of the relevant scaling laws which could be helpful in such studies cannot be evaluated completely until more experimental data are available. Therefore, any analysis, however elaborate, is likely to be inconclusive if its goal is the definition of a single, self-sufficient type of facility for investigation of low-density aerodynamics. Consistent with this view, the brief remarks in following sections dealing with various features of the tunnel are not intended to imply that all the relevant gas dynamic parameters are simulated, nor is there any attempt to prove that the compromises are necessarily optimum. However, preliminary experimental results, which are shown, indicate that this type of facility is capable of producing an environment having great utility for gas dynamic studies.

GENERAL DISCUSSION

SIMULATION

Although the subject will not be treated at length, it is appropriate to include a brief review of the flight simulation desired of the new facility and some of the compromises accepted. Several recent books and papers have defined the regimes of low-density flow in relation to hypervelocity flight (c. f. Refs. 1-5).

Manuscript released for printing August 1961.

Studies of flight in planetary atmospheres at high altitudes have disclosed that many of the most significant low-density aerodynamic phenomena occur in continuum fluid flow regimes. For example, Fig. 1 shows that important aerodynamic forces may be generated under conditions where decidedly complicated low-density phenomena occur, but that truly non-continuum flow is experienced mainly at orbital altitudes. The regimes of rarefied gas flow in Fig. 1 are defined for the stagnation region of a blunt body and follow Probstein (Ref. 5). The boundaries $1 \leq B \leq 1000$ encompass payloads being lowered by drag brakes and hypersonic gliders; contemporary missile warheads are somewhat above the upper bound.

Considerations of factors such as those presented in Fig. 1 led to the conclusion that flight at altitudes above 40 miles deserved special study because of pronounced low-density effects which are or will be encountered by re-entering bodies, hypersonic gliders, and future "space" planes" which may spend nearly 100 percent of their flight time above that altitude. Although velocities of 25,000 to 250,000 fps are of interest for interplanetary flight, no effort was made to produce such velocities. The reason is fairly obvious when the stagnation conditions corresponding to very high velocities are reviewed. Duplication of velocities encountered in space flight is not feasible by conventional wind-tunnel methods because of the extremely high stagnation enthalpies required. The related problem of producing and containing fluid at the necessary enthalpy levels is better appreciated when pressures and temperatures are considered. Figure 2 shows the isentropic stagnation conditions corresponding to the lower range of velocities. Practical difficulties facing the extension of conventional wind-tunnel methods of heating and then expanding gas to simulate the very high velocity conditions are evident in Fig. 2. First and foremost, the facility discussed herein was intended for low-density investigations with high speed but not necessarily the whole range of free-flight velocity duplicated.

Inasmuch as models tested in the prototype tunnel are small, Knudsen and Reynolds numbers are at least one order of magnitude different from full-scale vehicles in free flight at the same density. Because of the model's small size, in a low-density tunnel or firing range it is the same as a full-scale vehicle flying at much greater altitudes when Knudsen and Reynolds numbers are involved. Even though small model size does yield this compensation, caution must be exercised in exploiting the advantages of small models in low-density experiments because absolute scale may sometimes be a factor, for example, when reaction rates are slow.

The general velocity and density altitude regime of interest has been identified, and attention now will be turned to other factors which played a part in design of the facility.

SOME SIMULATION PARAMETERS

As a preliminary step in the design of the wind tunnel, consideration was given to the recognized simulation parameters associated with low-density flow. The object of this was, of course, to decide what characteristics the facility must possess to enable useful data to be gained. Stated another way, what must be duplicated, what can be simulated, and how serious is failure to satisfy fully some of the requirements? Since this report is written after the fact - i. e., the tunnel is already built - only the more significant decisions will be reviewed.

Mach Number and Velocity

Although it was deemed necessary that the flow be hypersonic, the question of velocity also arose. Obviously, hypersonic flow, requiring only stagnation temperature high enough to avoid liquefaction after expansion, meets some of the requirements and is easier to create in a wind tunnel. However, there are several points favoring high temperature or hypervelocity capability.

The great importance of wall heat transfer on such things as viscous interaction, and therefore the lift and drag of a large class of aerodynamic bodies, helped decide the issue in favor of high velocity and high temperature. This decision is supported by data such as those in Ref. 6 which compares aerodynamic forces and moments on wedges in low-density flow and demonstrates that the heat transfer condition is very important in determining aerodynamic forces. Obviously, approximation to free-flight boundary-layer conditions is closer if stagnation temperature is appreciably greater than wall temperature. Realization of this state of affairs can be aided by forced cooling of the model, as by circulating coolant internally, but this approach has obvious disadvantages for everyday testing. Also, the range of temperatures existing in the flow field around a model then would not be representative of free-flight. In that case, the changes in certain fluid characteristics occurring, for example, as a result of passage through a shock wave, would be different from free-flight (c. f. Ref. 7).

Further guidance favoring the choice of hypervelocity over merely hypersonic flow for low-density tunnels was found in the Mach number independence principle. As stated in the recent book by Hayes and Probstein (Ref. 4), that principle holds for the case of the strong shock, or $\left(M_\infty \sin \sigma\right)^{-2} \ll \epsilon_\infty$, and may be given as follows:

> "——a flow solution obtained for one sufficiently large value of M_∞ will serve for another large value of M_∞ if ρ_∞ and U_∞ are the same."

Duplication of ρ_∞ being an objective at the onset, this would indicate the desirability of high U_∞.

The ability to create and vary real fluid effects produced by high temperature appeared desirable because these effects were thought likely to require much study. This, then, was another point in favor of elevated temperature capability. Rather than study low-density and temperature sensitive phenomena separately in different facilities, a study of low-density alone or combined low-density and high temperature in a single facility seemed desirable.

Finally, the possibility of using the facility for nearly free-molecular flow experiments with very small, simple models was not overlooked. A need for such data obtained from high-speed flow exists, and it seemed probable that a hypervelocity facility could make useful contributions.

These are some of the reasons which led to the conclusion that not only hypersonic but also hypervelocity performance should be sought. This conclusion implies high stagnation enthalpy, and in a wind tunnel it also means supplying gas to the nozzle at high enthalpy. The associated problems are well known. Figure 3 shows a simple pressure-temperature relation summarizing the throat heat transfer situation. To the left on the figure, continuous operation of a wind tunnel is possible, but on the right only very brief run times are allowable. A boundary curve of constant throat heat flux has been drawn through a point representative of an advanced, continuous, hypersonic tunnel using indirect, water cooling. Thus, more elaborate cooling system design could be expected to move the curve to the right. A highly approximate indication of this is given by the line labeled future development which refers to a method of cooling by injecting a suitable fluid, e. g., helium, just upstream of the nozzle throat so that a blanket of cooling fluid forms a sub-layer along the nozzle surface. Application of this method may introduce serious flow abnormalities, however, and must be investigated more fully. Since structural problems of containing high pressure gas at high temperature have not been considered in drawing Fig. 3, some compromises might be necessary in specific applications. Although the pilot LDH Tunnel operates well to the left of the boundary in Fig. 3, these considerations and others briefly discussed later are presented because of their relevance to the future development of similar wind tunnels.

Knudsen and Reynolds Numbers

There was no need to make a decision as there was for the question of low or high velocity. It suffices to say that desired values of these parameters were those which would enable tests right in the middle of

the transition from continuum and essentially inviscid flow to free-molecular flow. Furthermore, it was believed preferable to achieve a condition of heat transfer to the models which would create relations between free stream and model wall temperatures similar to those applying in free-flight cases. Thus, the relations between free-stream and so-called "wall" values of Knudsen and Reynolds numbers also would be similar. The latter requirement contributed to the decision to design for high stagnation temperatures.

Thermodynamic Equilibrium

This subject must be regarded as part of a discussion of simulation when low-density, hypervelocity conditions are assumed. Unfortunately, the maintenance of thermal equilibrium is not always compatible with practical attainment of the flow conditions desired for investigation of other phenomena. For the flow to be in thermodynamic equilibrium as the fluid flows through a hypersonic nozzle, rapid adjustment in chemical composition and energy levels of vibrational, rotational, and translational degrees of freedom is required. Even though the different intervals of time characterizing the various reactions in the gas are extremely small by normal standards, high speeds and low densities may not give the time needed for the gas to adjust to rapidly changing conditions. In such cases, there is departure from equilibrium, and calculation of many fluid dynamic quantities is made difficult. Situations are known to arise where the adjustment lags to such an extent that the fluid may be considered effectively "frozen" insofar as its thermodynamic adjustments are concerned. In that case, a certain simplification in calculations results since the gas may be treated as a perfect gas with the ratio of specific heats determined by the particular condition of freezing. Thus, it often is possible to calculate the limiting conditions corresponding to equilibrium on the one hand and complete freezing of certain reactions on the other.

Theoretical effects of dissociated, non-equilibrium flow in wind-tunnel nozzles have been presented in various papers (c. f. Refs. 8-9). Similar effects pertaining to flow over aerodynamic bodies have been calculated (c. f. Refs. 10-11). Experimental results from measurements in a shock tunnel may be found in Ref. 12, and another example of a quantitative experiment on chemical non-equilibrium is discussed in Ref. 13. Other references may be found in the cited papers.

Effects of vibrational non-equilibrium, which may be encountered under less extreme conditions than dissociation, have been discussed in Refs. 14-18 and others.

Several monatomic gases are useful as working media in plasma heated tunnels. The main concern regarding thermodynamic equilibrium in such cases is directed to ionic recombination. Recent discussions of this subject are given in Refs. 19 and 20.

At the beginning of the work being described, there appeared to be good reasons to expect some degree of thermodynamic non-equilibrium, particularly when operating at the higher stagnation temperatures. The length and time available for readjustment of thermodynamic state before a particular station is reached by a molecule passing over a model is determined by model size if all the flow parameters are fixed. This implies that, all else being equal, no complete simulation of full-scale, free-flight exists short of complete duplication insofar as non-equilibrium thermodynamic processes are concerned. One may find slight comfort in remembering that complete simulation of full-scale, free-flight conditions rarely has been achieved in any aerodynamics laboratory in the past. But it does seem that the ability of the aerodynamicist to discover and distinguish between separate factors in his experiments receives its sternest test when low-density, hypervelocity laboratory experiments are undertaken.

The advent of significant thermodynamic non-equilibrium effects in aerodynamics laboratory work in the writers' opinion simply meant that it would require study by all means available. In the present case, it meant that one would have to consider the possibility and the effects of non-equilibrium in all experiments. This is equally true of free-flight testing, since all the non-equilibrium phenomena, including frozen flow, may occur there.

While on this subject it is worth remarking that very high Mach numbers (30-60) appear to be attainable by "frozen" expansions in plasma heated tunnels. However, one should not overlook the limit on attainable Mach number imposed by liquefaction or solidification of the gas medium. Figure 4 shows stagnation temperature required to keep test section temperature equal to 50°K, and Fig. 5 shows stagnation pressure required to keep test section pressure equal to one micron Hg. Air at one micron Hg solidifies at 35°K. Thus, the enchantingly high Mach numbers are not so easily reached using nitrogen or nitrogen-oxygen mixtures. However, if one uses gases with extremely low freezing points, such as helium, unusually high Mach numbers indeed appear attainable.

TYPE OF FACILITY

Various alternate paths of investigation may be followed in the development of a low-density facility. First, a shock-tunnel or "hotshot" tunnel

could be considered. Pumping rate of the vacuum pumps is not of major importance for such tunnels, and the short run times permit high reservoir pressures which enable expansions to high Mach numbers and very low pressures. Second, a ballistic range could also be considered. That type of facility appears to be the only one capable of simultaneous duplication of all hypervelocity stagnation conditions in air at fully defined ambient conditions. Third, a continuous, arc-heated wind tunnel limited to lower stagnation pressure than an intermittent tunnel by pumping rate and nozzle throat heat transfer limits also appeared to be worthy of study. Brief reviews of laboratory facilities of these types may be found in the literature (c. f. Refs. 21-23).

There are advantages associated with all classes of aerodynamic facilities listed above. It will only be stated that the continuous, arc-heated tunnel was chosen for further investigation because of its suitability for detailed, accurate experiments. This decision was reached with the benefit of the knowledge that both hotshot tunnels and hyperballistic ranges are in development at the von Karman Gas Dynamics Facility (VKF). Therefore, mutually advantageous interchange of test data is facilitated, and the individual types of equipment complement each other. In this case, the unfavorable features of a continuous tunnel, such as lower stagnation pressures and therefore greater susceptibility to thermodynamically frozen flow, may be balanced against the availability of supplemental data from associated facilities, and the well known advantages of continuous operation may be exploited.

DESIGN CONSIDERATIONS AND DESCRIPTION

A general view of the tunnel is presented in Fig. 6. Limited space prevented a more inclusive view, so such components as the power supply, gas storage, ejectors, cooling-water heat exchanger, and similar important accessories are not visible. These are indicated in the elevation view sketched in a highly simplified way in Fig. 7.

Usual operating conditions with the original nozzle fall within the indicated ranges when computed for flow in thermal equilibrium. These results are based on flow calibrations to be described later. The ranges are presented on the following page.

Gas ------ N_2 (other gases may be used)

Total temperature ------ 2000 - 4000°K (3600-7200°R)

Total pressure ------ 12 - 18 psia

Mach number ------ 9 - 11.4

Velocity ------ 7000 - 10,000 fps

Dynamic pressure ------ 2 - 4 psf

Unit Reynolds number ------ 220 - 420 per in.

Density ------ (2 to 4) x 10^{-6} lb/cu ft

Mean free path ------ approximately 1/10 in.

Equivalent density altitude ------ approximately 50 mi.

HEATER

A decision was made to use the heating scheme offering the highest temperatures and flexibility, yet not so advanced that a great deal of developmental research would be needed. The plasma generator or continuous arc-heater appeared to meet these specifications. Comprehensive, up-to-date reviews of plasma generators may be found in Refs. 24-25. A commercial unit was bought to avoid delay and the results of inexperience in plasma generator design.

A misconception appears to exist concerning Mach numbers to which a plasma-heated tunnel is limited by throat heating and arc chamber pressures. It has been said that Mach numbers of 7 or 8 represent the upper limit; however, the VKF prototype tunnel now operates at Mach numbers of 9 to 11.4, and this limit is imposed mainly by pumping capacity. An estimate indicates that methods well within present technology would enable Mach numbers over 20 to be reached in a continuous tunnel. Pumping capacity, nozzle boundary-layer growth, and gas liquefaction caused by low temperatures in the test section apparently represent the major limits on Mach number of plasma heated, continuous wind tunnels. On the other hand, stagnation pressures and temperatures certainly are limited by nozzle-throat heat transfer and arc-chamber strength. Heat losses arising from high arc-chamber pressures result in loss of efficiency, and the increased power required is another practical obstacle to attainment of high temperatures at high stagnation pressure.

The plasma generator used with the tunnel is a conventional, older, direct current design having a water-cooled, thoriated tungsten cathode

and water-cooled, copper anode. The gas to be heated flows axisymmetrically over the cathode and is constricted as it passes through the arc column and the combination nozzle and anode. Although it is nominally a 40-kw unit, the present tunnel consumes less than 20 kw under normal conditions. In its present form the plasma generator is reliable, and contamination of test section flow by electrode material has not been a problem with the nitrogen normally used as a test medium. Under normal operating conditions the plasma generator efficiency, line-to-gas, is approximately 60 to 65 percent.

One problem arising from the heating process is caused by the extremely high temperatures created in the gas issuing from the arc (≈ 10,000 - 50,000 °K). This raises questions concerning thermal equilibrium, reaction rates, the mechanisms of energy transfer, and even the definition of temperature (see e. g., Ref. 26). When the arc-heated gas discharges at pressures of an atmosphere or higher, local thermal equilibrium generally is assumed on the basis of spectroscopic measurements made at other laboratories.

SETTLING SECTION

The VKF low-density, hypervelocity (LDH) tunnel design incorporates a rather generously large settling chamber between the plasma generator and the entrance of the wind tunnel nozzle. This is intended to damp flow unsteadiness, encourage mixing, and promote thermodynamic equilibrium. Dimensions of this section are shown in Fig. 8. This originally was considered a temporary design, but it has been satisfactory and remains in use.

Naturally, a penalty in efficiency was expected because of heat loss from the gas in the settling chamber. For a typical case about 20 percent of the total input power or 30 percent of the power delivered to the settling chamber is lost there. The initial goal was merely to extend test capabilities into, first, low-density and, second, moderately high velocity conditions. The low weight-rate-of-flow made heating efficiency less critical. Planning of larger facilities obviously would be more affected by considerations of efficiency.

Temperature and impact-pressure surveys have been made inside the settling chamber with both heated and unheated flows. In the former case, the surveys could not be extended to the centerline because the probes could not withstand the great heat. Based on these tests, it appears that a pressure orifice in the settling chamber wall is satisfactory for measuring total pressure. Total temperature is determined by

measuring gas flow rate and pressure in the settling section. When the geometric area of the sonic section of the wind tunnel nozzle is known and when thermodynamic equilibrium is assumed, a temperature may be calculated using the continuity equation and the Mollier diagram for the gas. If it is assumed that the vibrational degrees of freedom of a diatomic gas, say N_2, are completely frozen in the settling section, a temperature roughly ten percent greater will be calculated when equilibrium T_o = 3020°K and p_o = 17.8 psia. When the calculated temperature for nitrogen is no greater than 3600°K dissociation is assumed to be negligible in the settling section where pressures are around one atmosphere. Most of the operations to date have been intentionally confined to undissociated flows. All total temperatures quoted herein are based on thermal equilibrium, measured total pressure and mass-flow rate, and known nozzle sonic throat area. Shift of the sonic station away from the section of minimum area because of heat transfer and skin friction has been calculated and found to be negligible.

Fluid from the arc heater, that is, the plasma, is electrically conductive. Conductivity of the fluid in the settling section has been measured and found to vanish upstream of the entrance to the nozzle.

A smaller settling chamber volume possibly would be satisfactory, particularly if the plasma generator were replaced with a design providing improved mixing in the plasma during the initial heating process in the arc chamber. Smaller wetted area would reduce heat loss from the contained gas.

NOZZLE

Design of the first nozzle for this wind tunnel was based on less secure grounds than present-day design of nozzles for more conventional tunnels. In the first place, the very conditions intended to be produced made the boundary-layer growth and viscous losses dominant in determining both nozzle contour and required pressure ratio. Secondly, performance of the pumping system was based entirely on calculated jet-ejector performance, so the relation between flow rate and tunnel "end" pressure was not known with certainty. Finally, it was planned to operate continuously with very high stagnation temperatures, which made design of the nozzle cooling system important. The fact that the original nozzle proved almost ideal attests to the good fortune attending these estimates.

Dimensions of the original nozzle are shown in Fig. 8. The conical expansion was adopted on the basis of estimated performance of other tunnel components and estimates of boundary-layer growth for expected

nozzle Mach and Reynolds numbers. Since these estimates indicated an approximately conical shape, the obvious machining ease decided the issue. Results of typical transverse impact pressure and "relative" total-temperature surveys in the original nozzle are shown in Fig. 9. The so-called "relative" total temperature was measured by a stagnation temperature probe of the type often used in unheated, supersonic flows. Thus, a greater part of the heat transmitted to the probe was lost through conduction and radiation, making the thermocouple output suitable only to indicate lateral distribution of heat flux at a given axial station in the nozzle. However, this information is valuable as a supplement to impact-pressure profiles. In this connection it is relevant to note that impact pressures are subject to increasingly large error as Reynolds number of the probe, $U_\infty D/\nu_\infty$, decreases below roughly 200. This feature undermines the usually high level of confidence associated with such probes. More will be said on this topic in a later section. Aside from the effect of low Reynolds number on impact-pressure probes, there is the well-known difficulty with impact-pressure probes in regions where large lateral gradients in Mach number and other quantities exist. Such conditions are typical of the edges of hypersonic boundary layers. Thus, even a merely "relative" total temperature may be more indicative of flow conditions at the edge of the core of uniform flow in the nozzle.

The impact-pressure probe used in obtaining the data shown on Figs. 9 and 10 was a water-cooled, flat-faced body of revolution having an outside diameter of 0.25 in. and an orifice diameter of 0.095 in. Profiles of both impact pressure and heat flux were found to be symmetrical about the nozzle axis.

Figure 9 reveals that the tremendous boundary-layer growth materialized as expected and showed that test section size of such wind tunnels really must be quoted in terms of "core diameter" to be meaningful. To take full advantage of the rather marginal pumping performance, the nozzle is designed to overexpand. Thus, a weak, reversed, conical shock emanates from near the exit of the nozzle. In a typical case this shock raises static pressure from about 15 microns Hg ahead of the shock to roughly 60 microns Hg downstream, thereby balancing pressure along the border of the hypersonic jet between nozzle exit and diffuser entrance. This is seen in Fig. 10 which shows three typical axial impact-pressure surveys. Location of the trailing shock depends on operating conditions, such as diffuser setting and model blockage. Its position is often made visible by the increased heating and red coloration locally on a sting or probe extending from the test section back through the shock.

A brief experiment has been conducted to find if extending the nozzle downstream causes a corresponding shift in shock position. To conduct

this experiment, two nozzle extensions were made. One was a right cylindrical tube with an inner diameter equal to nozzle exit diameter. The other was a crudely contoured replacement of the uncooled, downstream part of the basic nozzle, and its smaller diameter joined the basic nozzle at X = -5.8 in. Results shown in Fig. 11 will be helpful in designing a contoured nozzle for the tunnel. Only slight additional expansion is possible, but the exit shock can be moved about 6 in. downstream by extending the nozzle. Apparently this occurs because the higher tank pressure, p_t, influences boundary-layer development several inches upstream of the nozzle exit by transmission through the subsonic portion of the boundary layer.

Also apparent in Fig. 10 is the absence of any axial region of constant Mach number. This is not a serious matter because the Mach number gradient is not steep near the nozzle exit. However, a contoured nozzle now is being designed by a method appropriate to the flow characteristics. Studies of the calculation of nozzle boundary-layer thickness, δ, for cases where δ is of the order of nozzle radius were begun soon after the initiation of the low-density tunnel project. The method takes heat transfer and variable specific heats into account. The boundary layer in this nozzle has a typical laminar, hypersonic profile and is developed in the presence of a favorable wall heat-transfer condition, T_w/T_o being approximately 1/10.

The throat of the present nozzle remains relatively cool during tunnel operation. In a typical situation with total pressure 17.79 psia, total temperature 3020°K, and 3.6 lb/hr nitrogen flow rate, the entire nozzle cooling loss amounts to approximately 30 percent of the total input power to the heater.

TEST SECTION TANK

The 4-ft-diam tank enclosing the nozzle exit and diffuser inlet regions has no particular significance aerodynamically except that pressure in this tank is influential in determining strength and location of the shock wave trailing downstream from the nozzle. This pressure (p_t) may be adjusted and held constant when necessary by varying primary air pressure to one of the ejectors. Initial level of this pressure normally is determined by diffuser inlet location axially and blockage effect of the model or probe installed in the test section.

Size of the tank was dictated by space needed for easy installation of traversing mechanism, model and probe supports, instrumentation, and special experimental apparatus. Access to the interior normally is by

removal of the entire front flange which is supported by an overhead structure permitting the flange to be pushed back and forth with little effort. The heater, settling section, and nozzle all are mounted to this large flange and move with it.

Pressure transducers are mounted immediately adjacent to the nozzle exit inside the tank whenever possible. This reduces lag-time, which could be a serious problem in measuring pressures with long connecting tubing. Transducers are calibrated with the instruments exposed to the same ambient pressures and temperatures experienced during their subsequent use in a test.

DIFFUSER

A diffuser is a rather unusual component for a low-density wind tunnel. Because of the very pronounced viscous losses corresponding to the low Reynolds numbers throughout these tunnels, pressure recovery is poor and usually not especially attempted. However, even a small degree of recovery is valuable, and some effort toward that end was believed to be worthwhile. Therefore, the tunnel was designed so that various diffusers could easily be installed.

The first series of diffusers tested is described in Fig. 12. Design was rather arbitrary because of the absence of data for the combined low-density, hypervelocity flow conditions. As an economy measure, one entrance cone, one exit cone, and a series of central sections of varying diameters were fabricated from sheet metal. The smaller diameter central section had the greatest axial length, and each succeeding configuration of equal minimum diameter was made by cutting off part of the center section. Each succeeding diffuser of larger throat diameter was made by cutting off part of the conical sections so that their smaller diameters matched the new central section. Thus, the effect of central section length was investigated with entrance and exit section lengths constant for any given throat diameter, but the conical pieces became successively shorter with each increase in throat diameter.

Inasmuch as tank static pressure rather than tunnel pressure ratio was of direct concern in the present case, results are presented in terms of the tank pressure in Fig. 13. Examination reveals that variation of axial length of the constant area diffuser throats had negligible effect on tank pressure. However, diameter of this throat section is quite important. The apparent optimum value of unity for the ratio of nozzle exit and diffuser throat diameters probably is coincidental because much of the nozzle exit is filled with boundary layer. Free-jet length was a

factor in these tests, but it became less critical as the throat diameter was enlarged. When the latter dimension exceeded the optimum, influence of free jet length became relatively unimportant.

A review of the contributions of various segments of the diffusers is interesting. Figure 14 shows that a simple short-tube orifice in a wall reduced tank pressure from 60 to 30 microns Hg. Addition of a collector or convergent section further reduced tank pressure to 12 microns Hg. Completion of the diffuser by addition of the divergent section did not provide much additional benefit except when greater free jet lengths existed. It may also be noted that provision for a finite length of constant diameter throat resulted in an improvement over the performance of a convergent cone-frustum alone.

Rise in tank pressure resulting from blockage decreased as diffuser throat diameter increased. Figure 15 shows this for one set of operating conditions. The small size of the tunnel makes it important to minimize the size of supporting struts and other obstacles in the stream. The influence of tank pressure on position of the nozzle shock is indicated in Fig. 16. Benefits of the diffuser may be appreciated when it is realized that the axial spread of points in Fig. 16 covers approximately six useful test section diameters. A more extensive investigation of diffuser performance may be conducted in the future, but it is considered that the major gain already has been realized.

PUMPING SYSTEM

The pumping system consists of two stages of air injection plus the evacuation system of the VKF intermittent tunnels. The latter is an original part of the VKF plant, and in conjunction with a high pressure air storage vessel, it forms the drive system for two 12 in. tunnels. Access to the large vacuum tank and generous quantities of high pressure air were utilized in the low-density tunnel for economy. The vacuum tank may be evacuated to 0.04 - 0.10 psia (2-5 mm Hg) and maintained at that level for flow rates up to roughly 360 lb/hr. Although this capacity is vastly greater than necessary for the low-density tunnel, the pressures are not low enough. Therefore, two stages of a small, surplus steam ejector were cannibalized. Air from the VKF storage tank is used as the primary fluid for these ejectors because of its ready accessibility as compared to the added expense of providing steam. The ejectors lower the pressure at the tunnel to approximately 1/100 of that in the large, spherical vacuum tank into which the tunnel discharges. This pumping system has proved extremely satisfactory insofar as it is trouble-free and meets originally calculated performance.

RESULTS FROM INITIAL EXPERIMENTS

In view of the low densities, high speeds, and small size combined in this wind tunnel nozzle, there is a strong possibility of thermal non-equilibrium. On the basis of published reaction rates for nitrogen, both in regard to molecular vibration (Ref. 16) and dissociation (Ref. 20), it appears justifiable in the present case to assume equilibrium in the settling chamber just upstream of the nozzle. Then since little or no dissociation should exist in the nozzle under ordinary operating conditions, one may assume complete thermodynamic equilibrium and compute conditions in the test section on that basis. Alternatively one may assume freezing of vibrational degrees of freedom throughout the tunnel system and also compute test section conditions. Comparison of these latter calculations with results based on an equilibrium process should furnish some feeling for the possible uncertainty in flow parameters. The following is an example of these calculations for typical (equilibrium) reservoir conditions of 3020°K and 17.79 psia in nitrogen. Basis of the comparison is p_o'/p_o = constant in all flows..

	Equilibrium Flow	Vibration Frozen Throughout	Frozen at Throat
M_∞	= 9.4	10.5	10.4
U_∞, fps	= 8690	8270	7880
p_∞, microns Hg	= 19.8	15.4	15.4
T_∞, °K	= 190	143	129
ρ_∞, atm	= 3.9×10^{-5}	3.86×10^{-5}	4.25×10^{-5}
q_∞, psf	= 3.50	3.31	3.20
Re_∞ per in.	= 240	294	356

Evidence of vibrational non-equilibrium will be difficult to find because of the small differences in the quantities expected to exert the greater influence on measured data. In this example, it is interesting to note that the Reynolds number of consequence in tests of blunt bodies, Re_2, is about equal for equilibrium flow or either case of frozen flow. Another point of possible importance is the influence of contaminants on vibrational relaxation. There would seem to be a possibility that even extremely small amounts of foreign substances in the stream could significantly alter the conclusions one would draw from analyses based on reaction rates derived from tests with entirely "clean" fluids. Arc-heated hypervelocity tunnels, at best, produce slightly contaminated streams. Where necessary in the remainder of this discussion, a distinction between equilibrium and and frozen flows will be made. Unless stated otherwise, any flow parameters used later will be based on thermal equilibrium.

A photograph of a blunt model, similar to a Mercury capsule, installed in the LDH Tunnel is shown in Fig. 17. Flow visualization has been achieved by creating an electric field around the model through the mechanism of a difference in potential maintained by a Tesla coil.

The high temperatures encountered in this tunnel make it necessary to determine total enthalpy partially by indirect means. There is the possibility of energy losses between settling chamber and test section caused by viscous shear and heat transfer. This, as well as the question of thermodynamic equilibrium mentioned earlier, makes it particularly desirable to collect as many independent calibration data as possible. The most valuable data are those giving test-section conditions directly. In fact, if techniques for doing this were developed to a reliable state, the calibration of all types of high enthalpy tunnels would be far less dependent on assumptions and theoretical estimates.

It should be recognized that most of the flow-probing procedures commonly used in higher-density, lower-speed flows are not directly or easily applicable in low-density, hypervelocity streams. In this class fall static-pressure probes, total-temperature probes and shock angle or Mach line photography. Therefore, much time has been devoted to conducting and evaluating results from various calibration experiments designed to circumvent or at least account for viscous and thermal effects. Results of this work, in some cases preliminary in nature, are described in the following sections.

IMPACT-PRESSURE PROBES

The impact-pressure or pitot probe deserves its place at the top of this list because of its simplicity, the usually straight-forward interpretation of its readings, and most certainly because of its widespread use. Indeed, calculated flow parameters based on an impact pressure and assumed equilibrium or frozen isentropic expansion from partly measured and partly computed reservoir conditions often are considered sufficient tunnel calibration. First surveys of the LDH Tunnel nozzle were made by impact-pressure probes, but the verification of those results by independent measurements has been a goal.

After the time-consuming preparatory work directed toward simultaneous improvement of the tunnel and instrumentation as well as preliminary definition of flow conditions, a series of experiments was begun to establish the accuracy of the impact-pressure data. Two fundamental problems requiring attention were possible error caused by large thermal gradient along the probe and possible error from viscous effect at the

probe mouth. The first of these is discussed by Dushman (Ref. 27), Kennard (Ref. 28), and others. Howard (Ref. 29) has published useful experimental data. The second has been the subject of several investigations, particularly at the Universities of California and Toronto; see Sherman (Ref. 30), Chambre and Schaaf (Ref. 31), and Enkenhus (Ref. 32).

The error caused by temperature gradient also is a function of pressure level or Knudsen number. This has been established by experiments and is in agreement with the data of Ref. 29. Calibration surveys of the LDH Tunnel nozzle customarily are made with a water-cooled probe having an outside diameter of 0.25 in. and a bore diameter of 0.095 in. This standard probe, under the prevailing conditions, is not appreciably affected by thermal gradient. The thermal gradient correction could be appreciable for smaller impact probes or static-pressure probes, and it will be the subject of future research.

Shape of the head of the probe is a factor in determining the viscous effect, and because it was considered more convenient to use flat-faced probes in the LDH Tunnel, an investigation was conducted to establish the Reynolds number at which such influence is manifest. A summary of the earlier results is included in Fig. 18, where some data from other sources also are compared. It will be noted that the measurements involving the flat-faced or chamfered probes become affected at about equal Reynolds numbers, although the LDH Tunnel results correspond to a markedly higher Mach number and a moderately cooled wall condition of $T_w/T_o \approx 1/4$, compared to the other data for which $T_w \approx T_o$. The ratio, $T_w/T_o \approx 1/4$, could have been reduced by more elaborate cooling, but that was not thought to be necessary in this case. The correction of the LDH experimental data to account for the temperature gradient along the probe does not produce a significant change in the results, except at the lower Reynolds numbers. Thus, it is seen that little more than two-percent variation in impact pressure occurred even when $(UD/\nu)_\infty$ of the moderately cooled, flat-faced probes with $da/D \geq 0.7$ was reduced to 20. Data on the influence of other variables is being collected.

STATIC-PRESSURE PROBES

Measurement of free-stream static pressure in the LDH Tunnel is difficult because the very thick boundary layer on a conventional probe creates a spuriously high pressure at orifices located any practical distance from the stagnation point. Static pressure may be found by means of nozzle wall orifices, but there would be much doubt regarding radial pressure gradients associated with nozzles having large rates of increase of cross-sectional area and very thick boundary layers. Therefore, some

exploratory measurements have been made using a family of probes having conical noses and cylindrical afterbodies with orifice locations at varying distances downstream of the stagnation points. In doing this it was hoped that the pressure in the free stream could be found by extrapolating the pressure distribution along the probe to the limit of infinite length. Because of the perils of extrapolation processes, as well as other sources of possible error, the result is not regarded as infallible. On the other hand, free-stream static pressure is a useful supplement to other measurements which, taken all together, lead to sure definition of the flow conditions.

Since there is a thick boundary layer on the probes, it is assumed that the pressure distribution is determined largely by the displacement thickness. Where the growth of the displacement thickness is rapid, as it is at the orifice locations, pressure will be approximately proportional to the reciprocal of distance from the stagnation point x. as $x \rightarrow \infty$, the rate of change of p with $1/x$ will decrease. Therefore, we have chosen to plot static pressure against a parameter which contains x in the denominator so that the resulting curve should be linear throughout the region where most of the data points appear.

There is an axial Mach number gradient of 0.14 per inch for a typical case in the original, conical nozzle which has remained in use to the present time. Because their small size made it practical to measure pressure at only one distance from the tip on each probe, the probe tips were located at different axial stations in the nozzle while data were taken at a fixed nozzle station. In other words, a number of probes were used to get the pressure distribution, rather than a single probe with many orifices. Therefore, the Mach number and the pressure distributions on the forward portions of the probes varied slightly from probe to probe. Assuming pressures all along a probe were determined entirely by Mach number and pressure at the probe stagnation point, it is estimated that the axial gradient in the nozzle would cause static pressures measured with the minimum value of $1/x$ to be approximately 1.3 micron Hg high in relation to the pressure measured with the largest value of $1/x$. However, because this estimate did not include consideration of the effect of the nozzle free-stream gradient on boundary-layer growth, it probably is safe to conclude that the net effect amounted to less than one micron Hg. Because differences of that magnitude could be concealed in the experimental error, no correction is applied to the measured data. It is intended that additional study of static-pressure measurements will be taken up when the new, contoured nozzle is installed. Then, it is hoped, the axial gradient will not exist.

Another, even more important factor affecting the results is the correction to each probe reading necessitated by the high Knudsen numbers

in the probes and the temperature gradients along the probes. Whereas this was not significant in the impact-pressure measurements, the correction is responsible for 20 to 40 percent increases to the measured static pressures. In this case, the data of Howard (Ref. 29) have been used. Additional research on the effect of temperature gradient on measurement of very low pressures is being conducted.

Figure 19 shows three pressure distributions determined by the described method. A detailed discussion of these data is not justified before the axial-pressure gradient in the nozzle is eliminated and the effect of thermal gradient along the probe is determined more exactly. However, the results appear reasonably promising. The two upper curves presumably should coincide; and since they do not, inexact compensation for thermal gradient, nozzle pressure gradient, or differences in orifice geometry may be the underlying cause. When the data are extrapolated as shown, the end points fall between the equilibrium and wholly frozen flow pressures based on impact-pressure readings and assumed isentropic expansion from the settling chamber - i. e., p_o'/p_o. These are denoted by the thicker black bars on the ordinate; the tops of the bars represent thermal equilibrium, and the bottoms represent frozen vibrational modes throughout the system. Inasmuch as it is expected that the extrapolations should tend to level off as $1/x \rightarrow 0$, the true static pressures in both cases appear to be close to the equilibrium values. Unfortunately, the corrections for thermal gradient are so large that the data cannot be relied on to the degree necessary to prove or disprove thermal equilibrium. Even so, these results are valuable since the agreement with static pressures inferred from impact pressures points to the existence of isentropic flow in the nozzle. Another point possibly deserving notice is the decrease in pressures on the smaller probe at the smaller values of x (0.25 in.). Conceivably this could represent slip flow because $\left(M/\sqrt{Re_x}\right)_\infty = 1.2$ at this station.

Lateral traversing of a probe has shown constant static pressure across the core of uniform flow at the exit of the LDH Tunnel. When a tubular extension of 5.84 in. inside diameter is connected to the nozzle exit so that the conical nozzle is followed by about 12 in. of constant area duct, the higher tank pressure does not influence the boundary layer so strongly at the exit of the conical nozzle. Then, an investigation with $T_o = 3020°K$ shows that static pressure computed from centerline impact-pressure ratio, p_o'/p_o, and based on thermal equilibrium closely agrees with static pressure taken from an orifice in the wall of the nozzle at the corresponding axial station.

MASS-FLOW PROBE

As part of the extended calibration program demanded by the low-density, hypervelocity character of the nozzle flow, a mass-flow probe was tested. The idea certainly is not new, but successful application seems to be rare. There are several points at which failure may occur in attempting to measure local mass-rate-of-flow, but the possibility of deriving valuable data from the experiment encouraged the present effort. Obviously, if the product $(\rho U)_\infty$ can be measured by a mass-flow probe, this can be compared to the value computed on the basis of impact-pressure measurements, and agreement would constitute strong proof of the accuracy of all other calibration data based on isentropic nozzle flow. Also, when hypersonic flow impact pressure $p_o' \approx (\rho U^2)_\infty$, one may obtain approximate ρ_∞ and U_∞ directly from impact and mass-flow probe measurements.

A schematic diagram of the equipment used is shown in Fig. 20, and the sequence of operation follows:

1. The probe tip is positioned at the point where the local quantity $(\rho U)_\infty$ is to be measured.
2. Ideally, with valves 1, 3, and 6 open, the flow in a stream tube equal in area to the probe opening is swallowed into the probe. (Valves 2, 4, and 5 initially are closed.)
3. Valves 4 and 5 are manipulated to position the oil levels at A--A' and then left closed.
4. Needle valve 6 is adjusted so that the pressure above the oil level at A is increased to a conveniently measurable value but is still low enough to ensure that the flow ahead of the probe tip is swallowed.
5. The pressure at the micromanometer and the oil height in the sight glass are noted.
6. Valve 3 is closed simultaneously with the opening of valve 4, and the time is noted. The oil level then begins to drop, providing space for the mass flow from the probe.
7. Valve 4 is closed so that the oil level will stabilize at levels B--B'. The pressure above the oil is now less than the initial pressure because of the increased volume. The pressure is increasing because of the incoming flow.
8. When the pressure indicated on the micromanometer is the same as that noted in step 5, valve 1 is closed, valve 2 opened, and the time again noted.

9. The mass-flow through the probe is given by the equation

$$\dot{m}_1 = \rho_v \Delta V/\Delta t$$

If,
$$\dot{m}_1 = (\rho U)_\infty A_p, \quad (1)$$

then
$$(\rho U)_\infty = \rho_v \Delta V/(A_p \Delta t) \quad (2)$$

Also feasible is a second approach wherein the oil is omitted and the tank merely allowed to rise from a very low initial pressure to some limiting higher pressure as mass is passed into it. Of course, it must be determined that mass-flow-rate is not variable with pressure during this process.

The most crucial factor in this experimental procedure is the swallowing of the shock wave at the probe inlet. If the shock is not swallowed, effective inlet area is not equal to geometric area, and the measurement is useless unless some form of calibration can be devised. Using the type of equipment described herein, one could plot local mass-flow rate as a function of p_v and find a value of p_v below which $\dot{m}_1$ becomes constant. In practice, however, the combination of limited tank size and narrow useable range of p_v's prevented full application of this checking technique. The system is being improved so that more thorough investigations can be made. Investigation by varying p_v indicates that the shock was nearly, but not completely, swallowed when the probe inlet was near the nozzle exit. Complete swallowing is believed to have been accomplished upstream of X = -3 for T_o = 3020°K and upstream of X = -5 for T_o = 2220°K. Results of the first measurements are presented in Fig. 21.

MEASUREMENTS OF DRAG OF SPHERES

In earlier days, sphere drag was used as a wind tunnel calibration test for determining stream turbulence. Sphere drag measurements have also gained an established place in low-density wind-tunnel work. In this connection, such data serve to extend knowledge of aerodynamic drag and also to aid in tunnel calibration by enabling comparison of data taken from various tunnels. A limited series of measurements has been completed using the LDH Tunnel.

A water-cooled, axial-force balance permitting measurement of loads in the range from 0.002 to 0.015 lb was used. This balance was built for another purpose and was used for the measurement of sphere drag because of its availability. As a result, the range of measurements was limited, but none the less useful. The spheres were of solid steel

and were maintained at surface temperatures T_w approximately equal to 0.3 total temperature T_o. Mach number was 9.4, and unit Reynolds number was 240 per inch.

To compare data from various sources, a means of approximate correlation was attempted. If drag coefficients are plotted against a form of Reynolds number, such as Re_2, data obtained from tests in hypervelocity streams with $T_w \ll T_o$ will not agree with data from tests where $T_w \approx T_o$ and $M_\infty < 5$ because both the drag coefficients C_{Dc} at high Reynolds numbers and the free-molecular flow drag coefficients C_{Dfm} will be different. This obstacle to the comparison of data is largely eliminated by using the quantity $(C_D - C_{Dc})/(C_{Dfm} - C_{Dc})$ as the dependent variable. When presented in this form, variations in C_D caused by differences in Mach numbers, temperatures, and heat transfer tend to vanish. The data of Hodges (Ref. 33) may be used to obtain C_{Dc}. As a convenience, the faired data curve from Ref. 33 is reproduced here in Fig. 22. The free-molecular drag coefficients for spheres, assuming completely diffuse reflection of incident molecules is given in Ref. 34 as

$$C_{Dfm} = \frac{e^{-S^2/2}}{S^3\sqrt{\pi}}(1 + 2S^2)\frac{4S^4 + 4S^2 - 1}{2S^4}\operatorname{erf}(S) + \frac{2\sqrt{\pi}}{3S_w} \qquad (3)$$

where

$$S = U_\infty / \sqrt{2RT_\infty} \qquad (4)$$

$$S_w = U_\infty / \sqrt{2RT_w} \qquad (5)$$

Following this procedure, Fig. 23 has been prepared. In this case

$$Re_2 = (U/\nu)_2 D \qquad (6)$$

and all quantities pertaining to the LDH Tunnel are based on flow in thermodynamic equilibrium. Inspection of the result leads to the conclusion that data from the LDH Tunnel are consistent with other published measurements. This tends to substantiate the nozzle calibration based on surveys with probes discussed previously.

REFERENCES

1. Lees, Lester. "Recent Developments in Hypersonic Flow." Jet Propulsion. Vol. 27, No. 11, November 1957, pp. 1162-1178.

2. Liepmann, H. W. and Roshko, A. Elements of Gas Dynamics. John Wiley and Sons, New York, 1957, pp. 380-382.

3. Adams, Mac C. and Probstein, Ronald F. "On the Validity of Continuum Theory for Satellite and Hypersonic Flight Problems at High Altitudes." Jet Propulsion, Vol. 28, No. 2, February 1958, pp. 86-89.

4. Hayes, Wallace D. and Probstein, Ronald F. Hypersonic Flow Theory. Academic Press, New York and London, 1959, pp. 375-386.

5. Probstein, Ronald F. "Shock Wave and Flow Field Development in Hypersonic Re-entry." (Preprint) Presented at the American Rocket Society Semi-Annual Meeting, Los Angeles, May 9-12, 1960.

6. Schaaf, S. A., Moulic, E. S., Chahine, M. T., and Maslach, G. F. "Aerodynamic Characteristics of Wedges in Low Density Supersonic Flow." (Preprint) Presented at the American Rocket Society Semi-Annual Meeting, Los Angeles, May 9-12, 1960.

7. Hammitt, Andrew G. "Dimensionless Parameters for Viscous Similarity." Jour. Aero. Sci., Vol. 27, No. 9, September 1960, p 720.

8. Bray, K. N. C. "Departure from Dissociation Equilibrium in a Hypersonic Nozzle." British A.R.C. 19, 983, March 1958.

9. Hall, J. G. "Studies of Chemical Non-Equilibrium in Hypersonic Nozzle Flows." C.A.L. Report 1118-A-6; AD 229131, November 1959.

10. Bloom, M. H. and Steiger, M. H. "Inviscid Flow with Non-Equilibrium Molecular Dissociation for Pressure Distributions Encountered in Hypersonic Flight." Jour. Aero. Sci., Vol. 27, No. 11, November 1960, pp. 821-835.

11. Whalen, Robert J. "Viscous and Inviscid Non-Equilibrium Gas Flows." I.A.S. Paper No. 61-23, January 1961.

12. Nagamatsu, H. T., Geiger, R. E., and Sheer, R. E., Jr. "Real Gas Effects in Flow over Blunt Bodies at Hypersonic Speeds." Jour. Aero. Sci., Vol. 27, No. 4, April 1960, pp. 241-251.

13. Wegener, Peter P. "Experiments on the Departure from Chemical Equilibrium in a Supersonic Flow." Amer. Rocket Soc. Jour. Vol. 30, No. 4, 1960.

14. Kantrowitz, Arthur. "Effects of Heat Capacity Lag in Gas Dynamics." Letter to the Editor, Jour. of Chem. Physics Vol. 10, No. 2, February 1942.

15. Kantrowitz, Arthur. "Heat Capacity Lag in Gas Dynamics." Jour. of Chem. Physics, Vol. 14, No. 3, March 1946.

16. Blackman, Vernon. "Vibrational Relaxation in Oxygen and Nitrogen." Journal Fluid Mech., Vol. 1, Pt. 1, May 1956, pp. 61-85.

17. Stephenson, Jack D. "A Technique for Determining Relaxation Times by Free-Flight Tests of Low-Fineness Ratio Cones; with Experimental Results for Air at Equilibrium Temperatures up to 3440°K." NASA TN D-327, September 1960.

18. Sedney, Raymond. "Some Aspects of Non-Equilibrium Flows. Jour. Aero. Sci., Vol. 28, No. 3, March 1961, pp. 189-196, 208.

19. Bray, K. N. C. and Wilson, J. A. "A Preliminary Study of Ionic Recombination of Argon in Wind Tunnel Nozzles." Univ. of Southhampton, U.S.A.A. Rept. No. 134, February 1960.

20. Wray, K., Teare, J. D., Kivel, B. and Hammerling, P. "Relaxation Processes and Reaction Rates behind Shock Fronts in Air and Component Gases." Avco Research Laboratory, Res. Rept. 83, December 1959.

21. Lukasiewicz, J. "Experimental Investigation of Hypervelocity Flight." First International Congress of the Aeronautical Sciences, ICAS, Madrid, 1958.

22. Henshall, B. D. "A Review of the Development of High Enthalpy Aerodynamic Test Facilities." Applied Mech. Reviews, Vol. 13, No. 6, June 1960.

23. Warren, Walter R. "Laboratory Experimental Studies in Re-entry Aerothermodynamics." Tenth International Astronautical Congress, London, 1959.

24. John, Richard R. and Bade, William L. "Recent Advances in Electric Arc Plasma Generation Technology." Amer. Rocket Soc. Jour., Vol. 31, No. 1, January 1961.

25. Materials Advisory Board, National Academy of Sciences. "Development and Possible Applications of Plasma and Related High-Temperature Generating Devices." Rept. MAB-167-M, August 1959.

26. Hill, William W., Jr., and Stanley, Paul E. "Instrumentation Studies for Plasma Jet and Hypersonic Wind Tunnel" Purdue Res. Foundation Rept. No. A-59-12, August 1959.

27. Dushman, Saul. Scientific Foundations of Vacuum Techniques. John Wiley and Sons, Inc., New York, 1949, pp. 65-67.

28. Kennard, Earle H. Kinetic Theory of Gases. McGraw-Hill Book Co., Inc., New York, 1938, pp 327-333.

29. Howard, Weston M. "The Effect of Temperature on Pressures Measured in a Hypersonic Wind Tunnel." J. Aero/Space Sci., Vol. 26 No. 11, November 1959, p. 764.

30. Sherman, F. S. "New Experiments on Impact Pressure Interpretation in Supersonic and Subsonic Rarefied Air Streams." Univ. of California Institute of Engr. Res. Rept. No. He-150-99, December 21, 1951.

31. Chambre, P. L. and Schaaf, S. A. "The Impact Tube." Physical Measurements in Gas Dynamics and Combustion. Princeton University Press, 1954, pp. 111-123.

32. Enkenhus, K. R. "Pressure Probes at Very Low Density." Institute of Aerophysics, Univ. of Toronto, UTIA Rept. No. 43, January 1957.

33. Hodges, A. J. "The Drag Coefficient of Very High Velocity Spheres." J. Aero. Sci., Vol. 24, No. 10, October 1957, pp. 755-758.

34. Schaaf, S. A. and Chambre, P. L. "Flow of Rarefied Gases." Fundamentals of Gas Dynamics. Princeton University Press, 1958, p. 704.

35. Kane, E. D. "Drag Forces on Spheres in Low Density Supersonic Gas Flow." Univ. of California Institute of Engr. Res. Rept. No. HE-150-65, February 15, 1950.

36. Sreekanth, A. K. "Aerodynamic Force Measurements in a Highly Rarefied Gas Stream." in Bulletin and Annual Progress Report 1960. Institute of Aerophysics, Univ. of Toronto, October 1960, pp. 12, 69, 70.

37. Wegener, Peter P. and Ashkenas, Harry. "Wind Tunnel Measurements of Sphere Drag at Supersonic Speeds and Low Reynolds Numbers." Jet Prop. Lab., California Inst. of Tech., Tech. Release No. 34-160, November 25, 1960.

38. Masson, D. F., Morris, D. N., and Bloxsom, Daniel E. "Measurements of Sphere Drag from Hypersonic Continuum to Free Molecular Flow." Rand Corp. Res. Memo. RM-2678, November 3, 1960.

ACKNOWLEDGMENTS

A project involving the design, construction, and testing of a new wind tunnel, even though it is small, normally is supported by the work of many persons. The present case is an example of this, and it is impossible to acknowledge every deserving person by name. Therefore, only those who have been most active throughout the entire project can be recognized specifically. They are David E. Boylan, Betty M. Majors, R. F. Armstrong, R. L. Beavers, J. M. West, Jack A. Durand, J. M. Ford, and Leona K. Meeks.

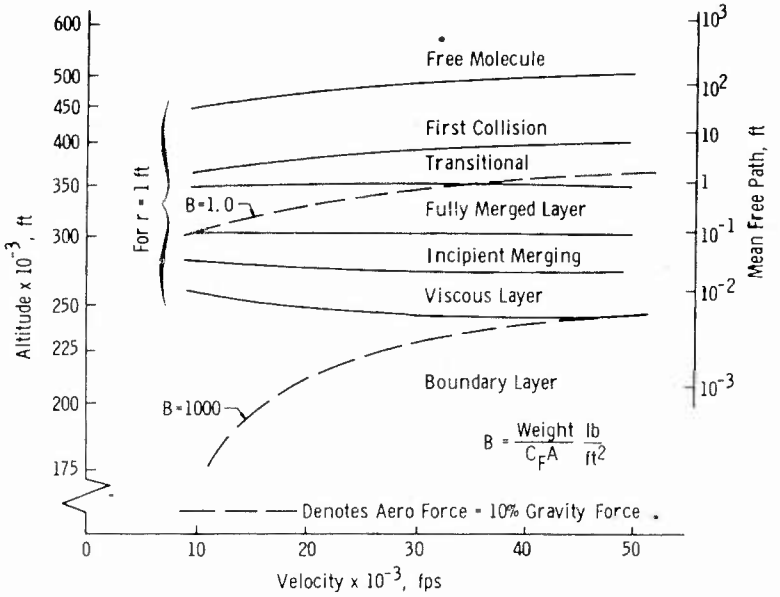

Fig. 1 Regimes of Low-Density, Hypervelocity Flow Defined for the Stagnation Region of a Blunt, Cooled Body in the Earth's Atmosphere (See Ref. 5)

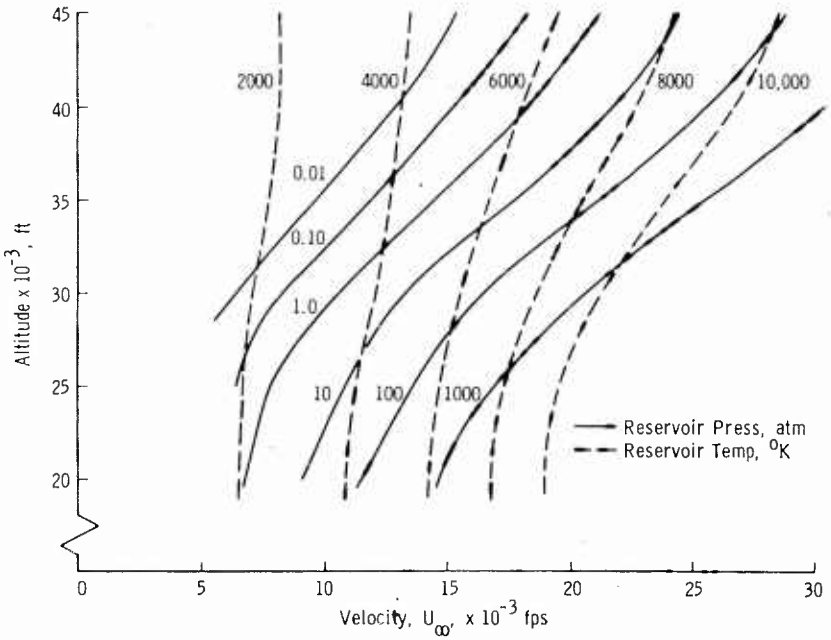

Fig. 2 Isentropic Stagnation Conditions for Equilibrium Air

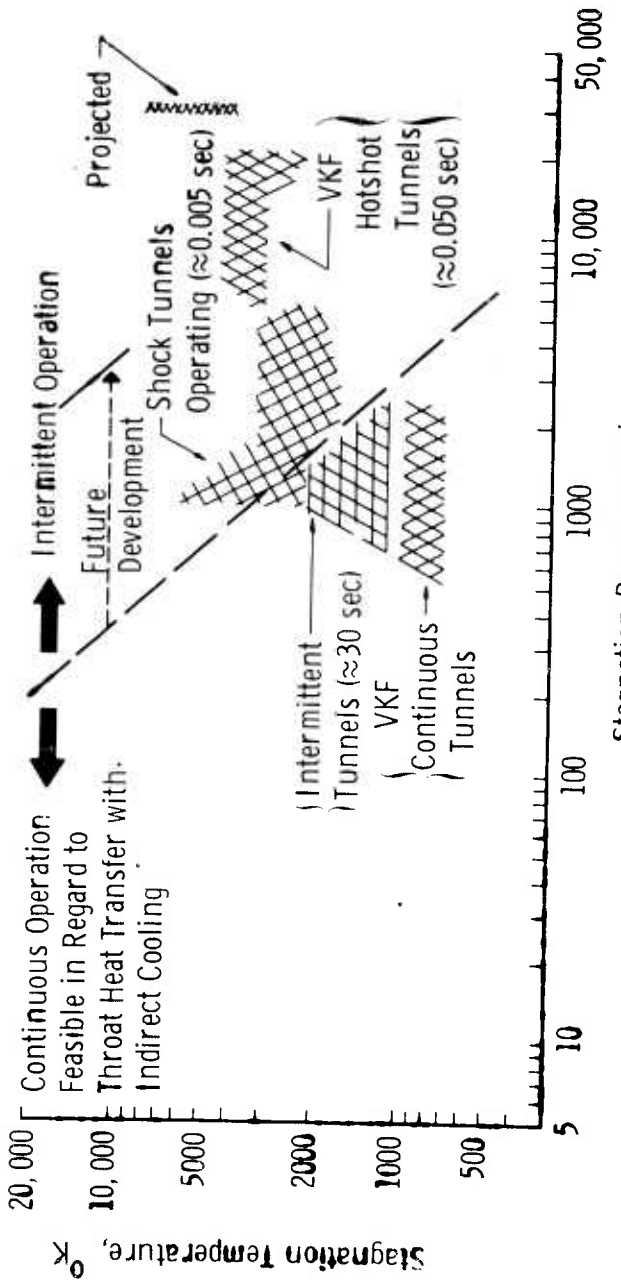

Fig. 3 Approximate Limits Imposed on Conventional Wind Tunnels by Throat Heating Alone

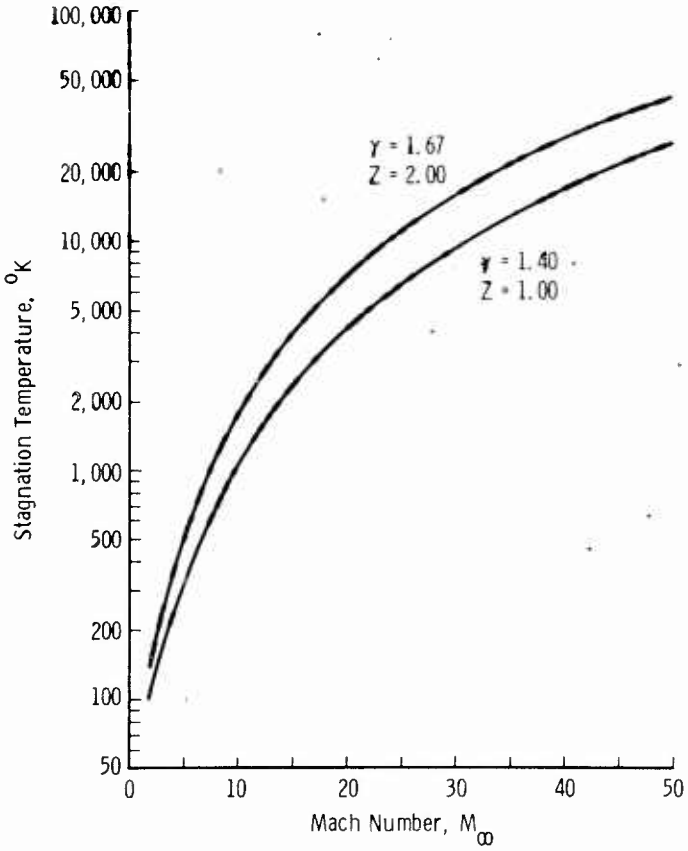

Fig. 4 Reservoir Temperature Required to Maintain Test Section Temperature of 50°K

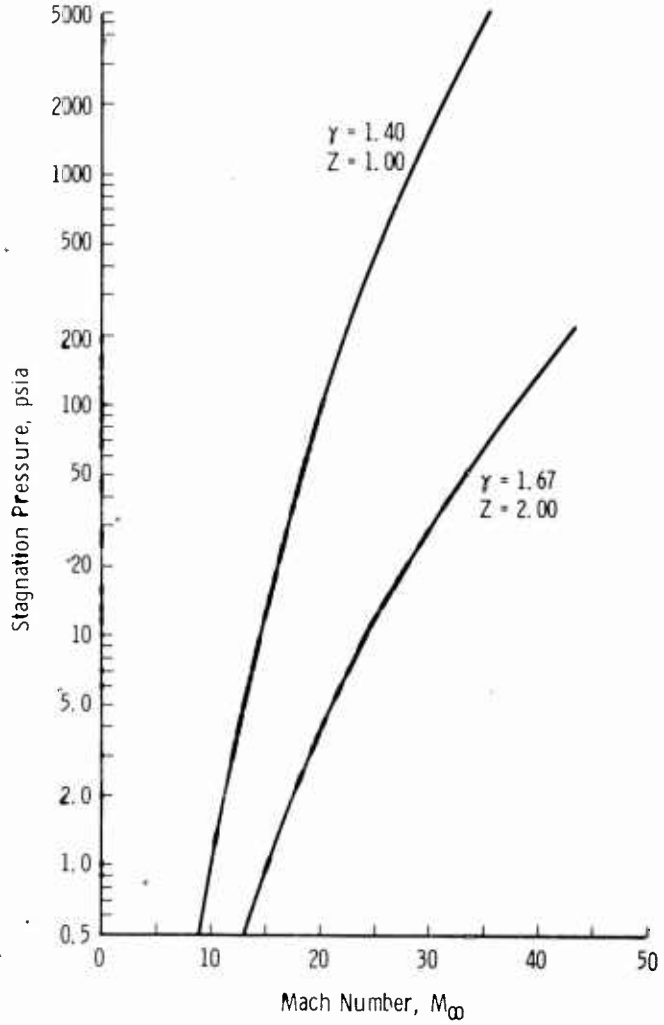

Fig. 5 Reservoir Pressure Required to Maintain Test Section Pressure of 1 micron Hg

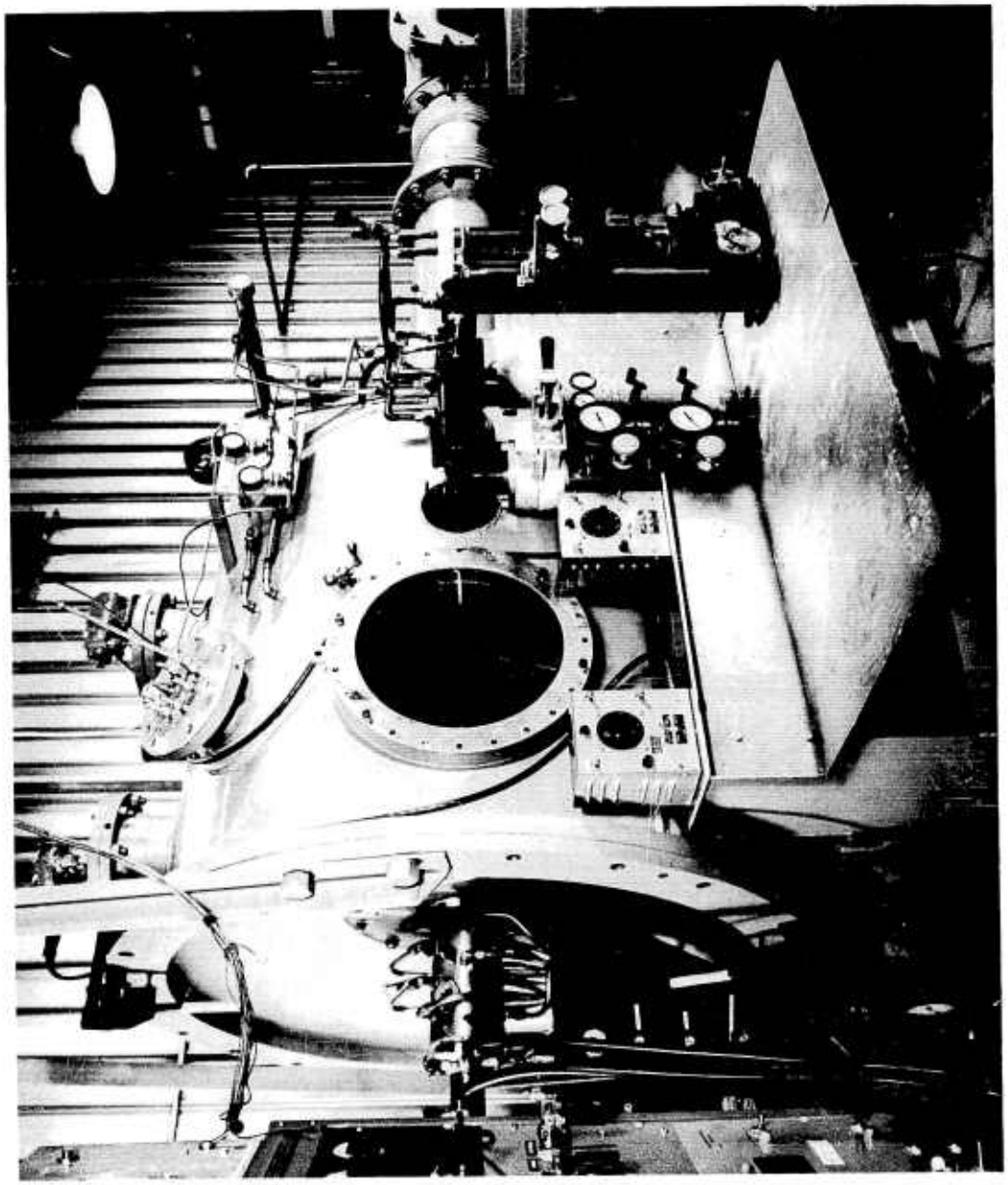

Fig. 6 Photograph of Low-Density, Hypervelocity (LDH) Wind Tunnel of the von Karman Gas Dynamics Facility, USAF Arnold Center

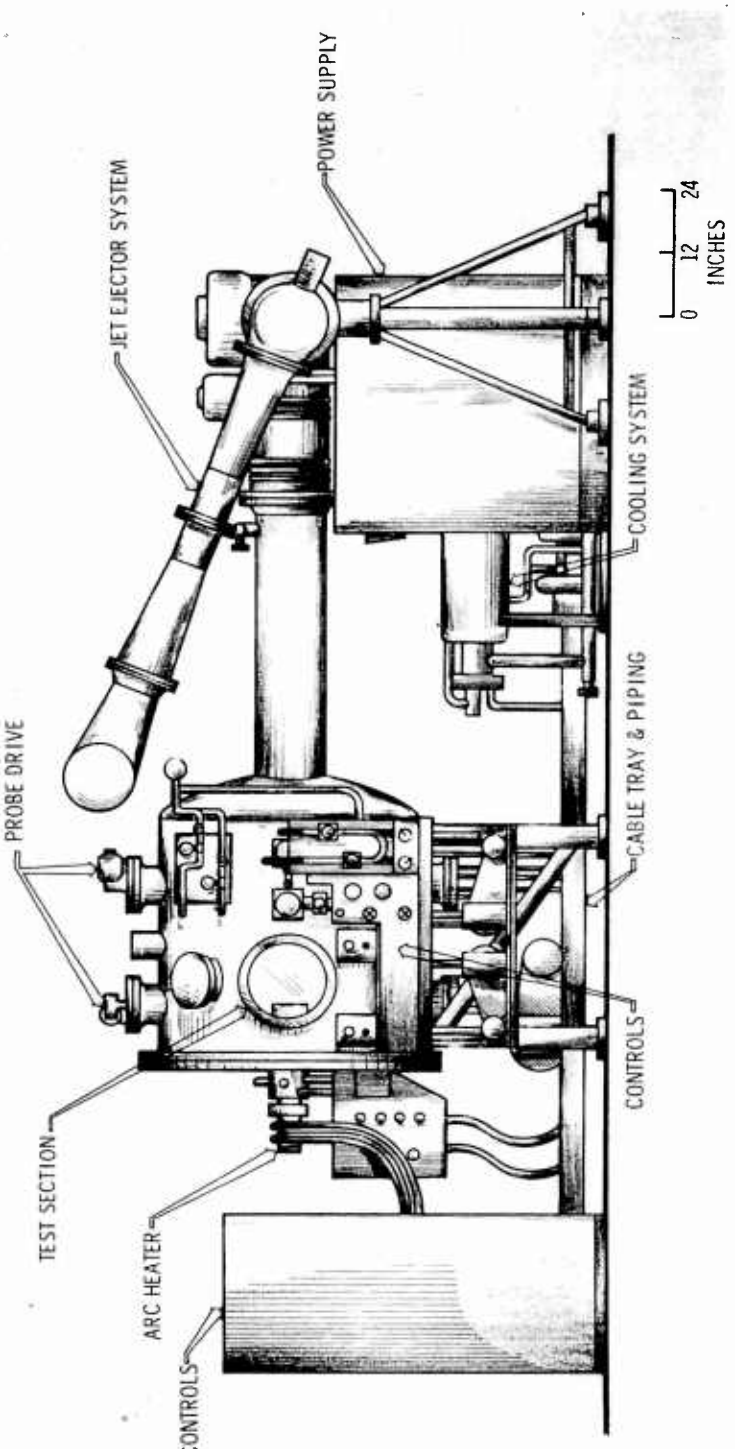

Fig. 7 Elevation View of the LDH Wind Tunnel with Major Components Identified

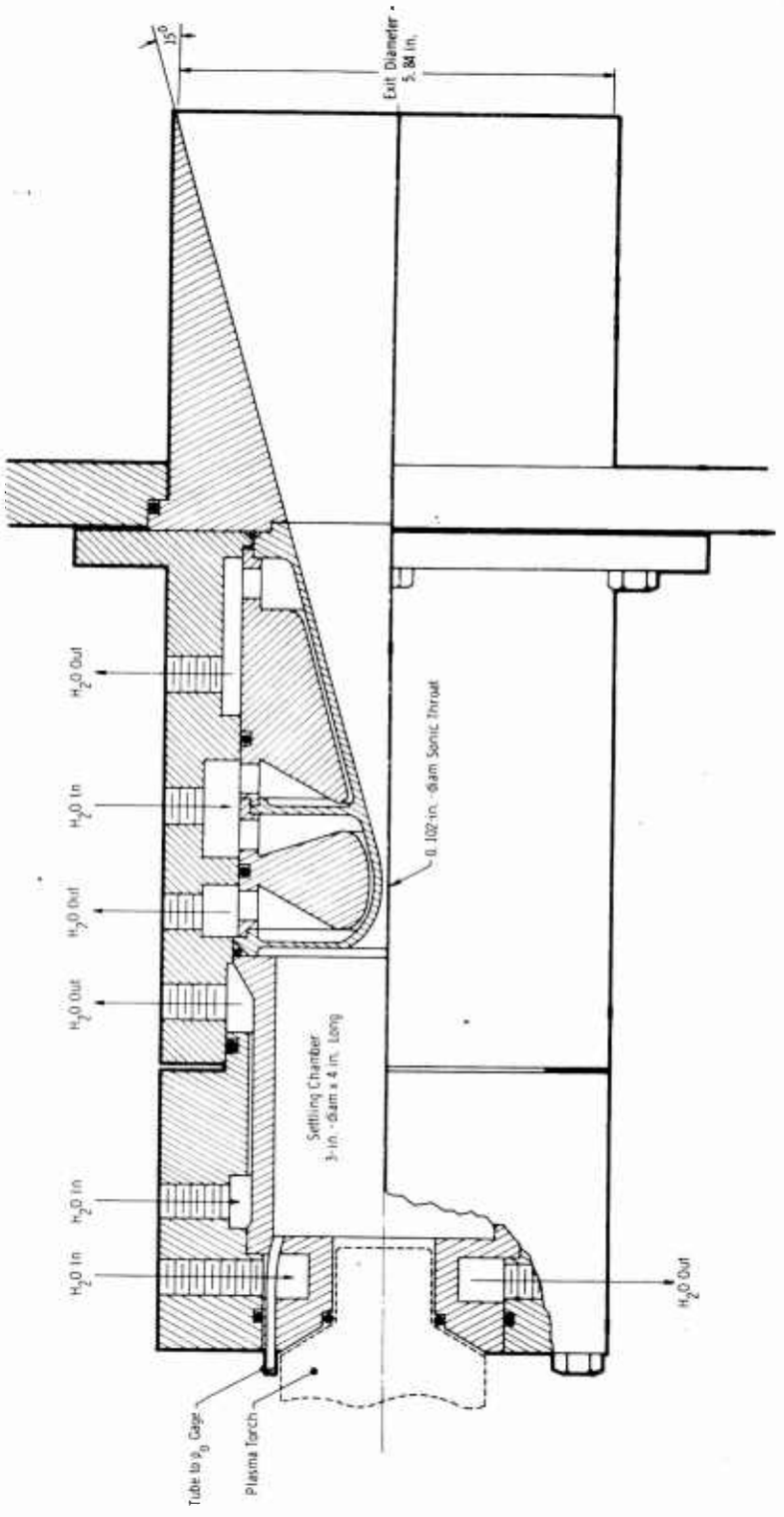

Fig. 8 Nozzle and Settling Chamber

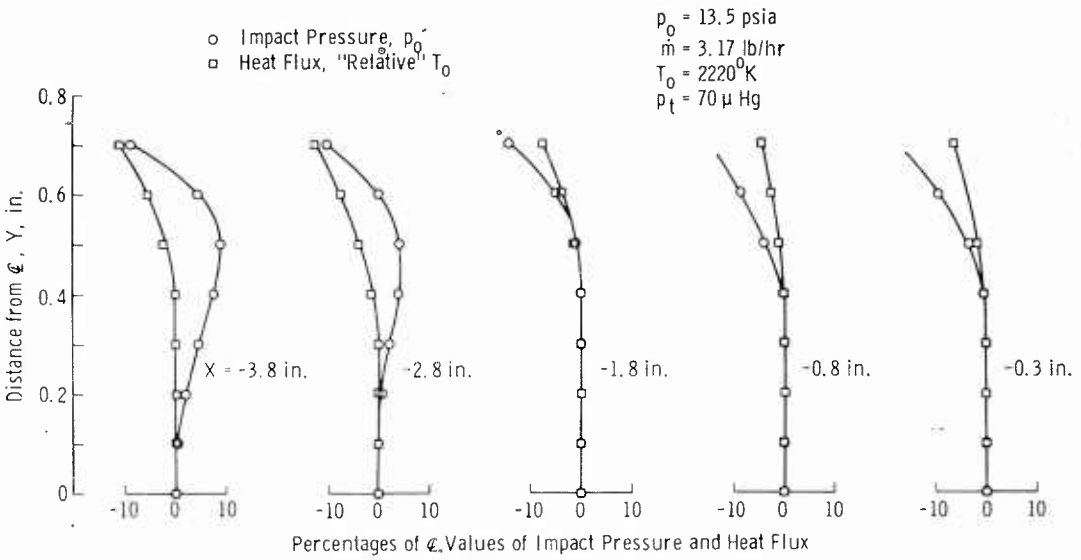

Fig. 9 Typical Results of Transverse Surveys at Various Axial Stations in the LDH Tunnel Conical Nozzle (Total Angle = 30 deg)

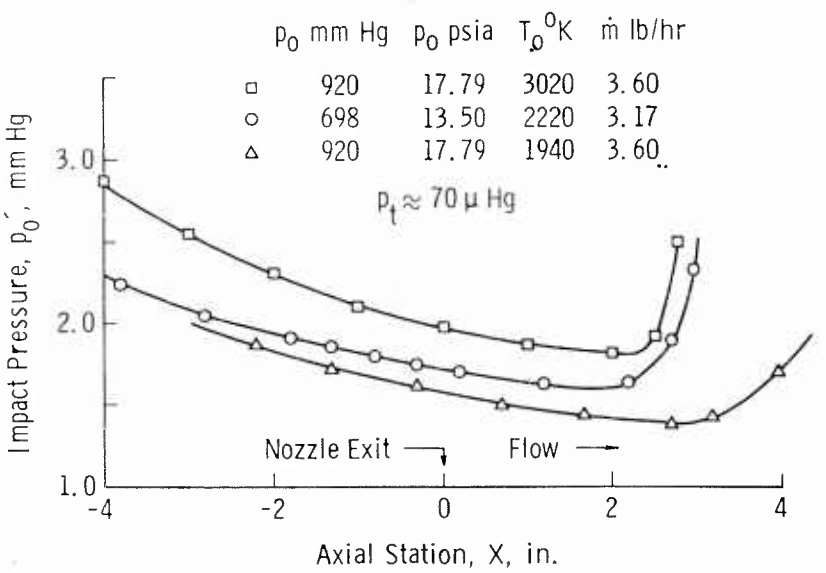

Fig. 10 Axial Centerline Impact-Pressure Distributions

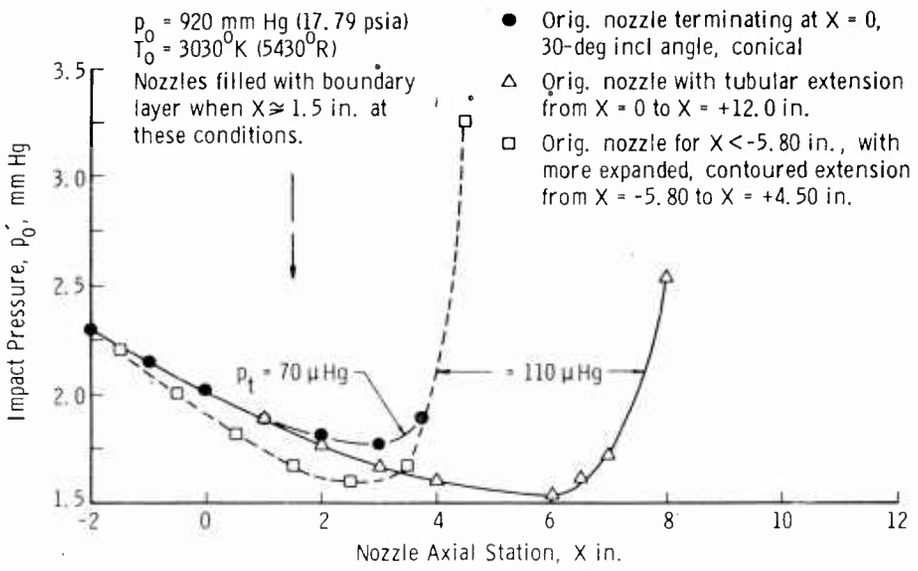

Fig. 11 Centerline Impact Pressures with Extensions Added to the Original Nozzle

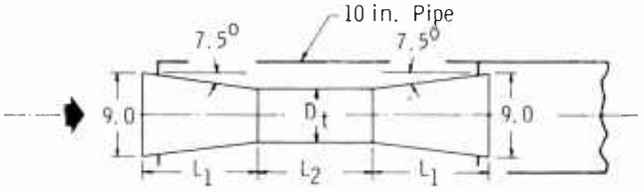

Dimensions in inches and degrees

Diffuser	L_1	L_2	D_t	Notes
1A	15	24	4.8	
1B	15	13.25	4.8	
1C	15	8.25	4.8	
2A	14	23.5	5.2	
2B	14	14	5.2	
2C	14	6	5.2	
3A	13	23.3	5.6	
3B	13	13.3	5.6	
3C	13	5	5.6	
4A	10.5	0	6	Convergent section only
4B	10.5	6	6	Convergent and throat sections
4C	0	6	6	Throat section only
4D	10.5	5.5	6	Complete diffuser
5A	9	5.875	6.375	

Fig. 12 Diffuser Configurations

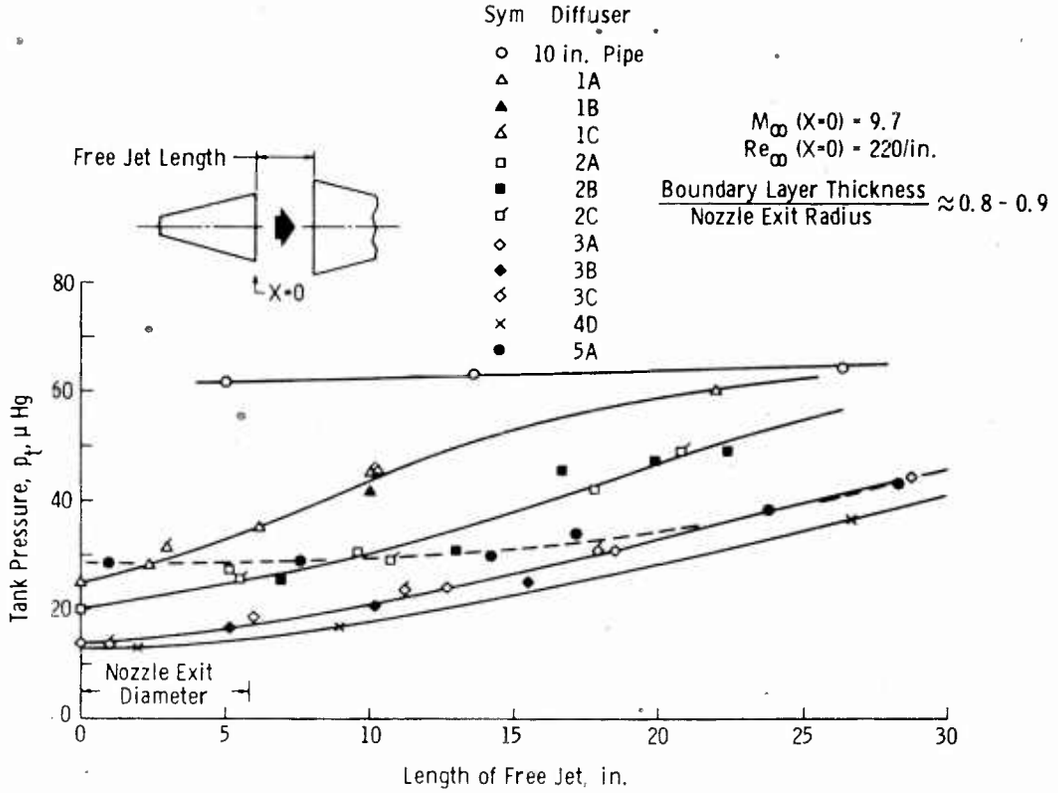

Fig. 13 Diffuser Performance with Clear Jet

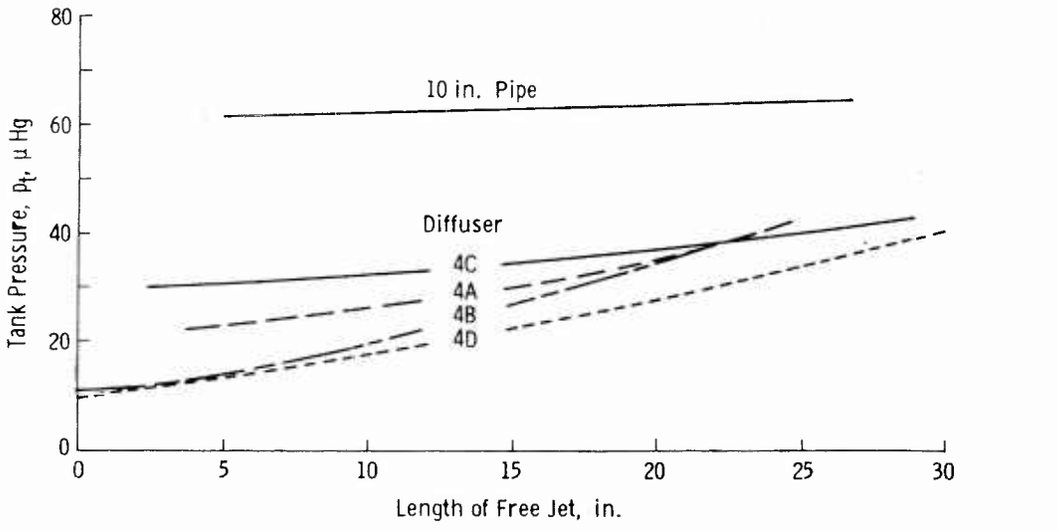

Fig. 14 Diffuser Component Contributions with Clear Jet

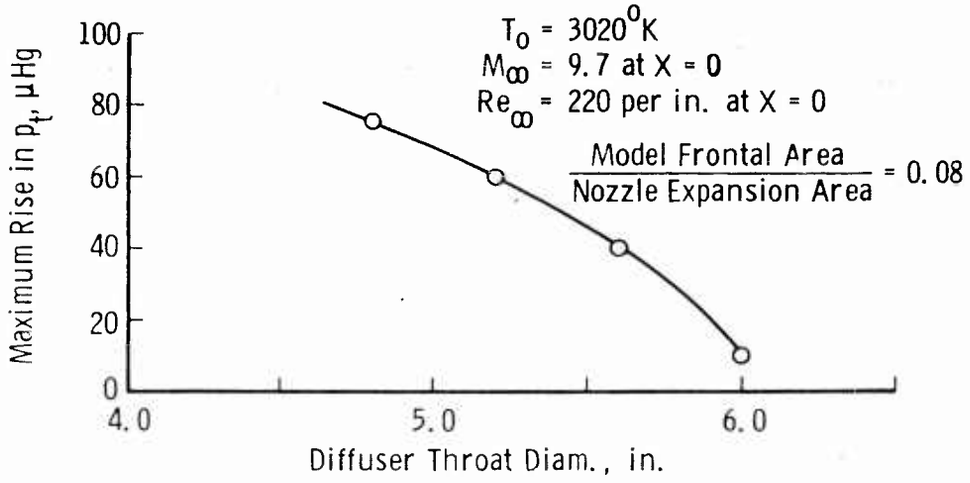

Note: Nozzle expansion area = Cross-sectional area at exit minus area of displacement boundary layer at exit. Model was circular cylinder normal to flow, and frontal area is taken as that portion not covered by the nozzle displacement boundary layer.

Fig. 15 Effect of Blockage on Tank Pressure, p_t

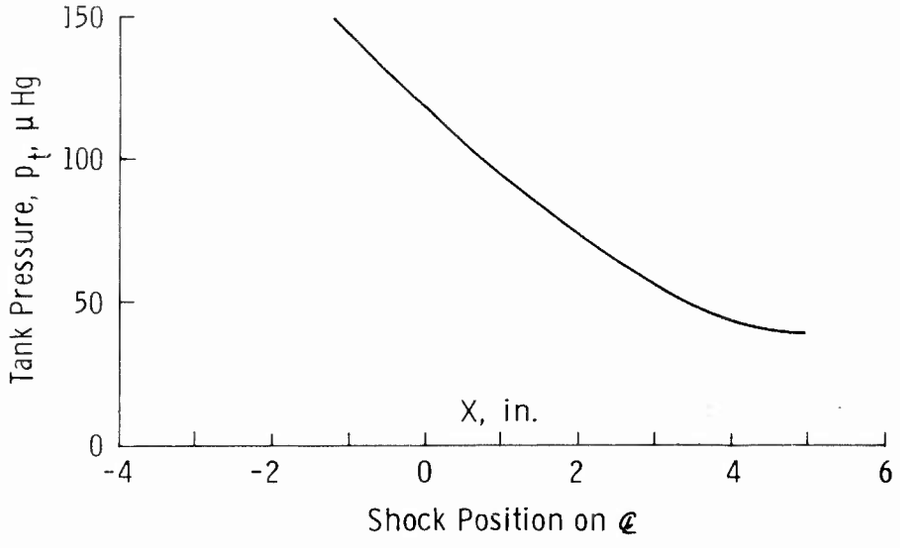

Fig. 16 Effect of Tank Pressure on Shock Position

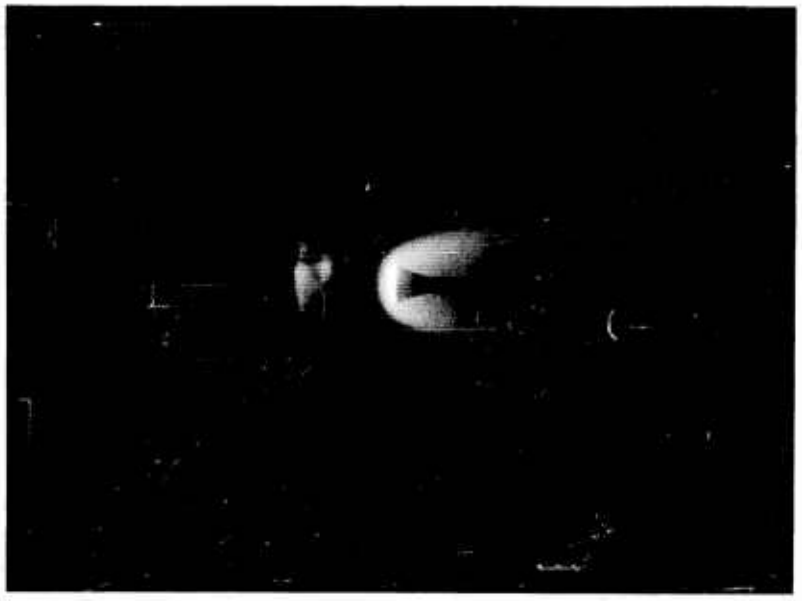

Fig. 17 Flow Visualization Produced by Artificially Created Electric Field, $M_\infty = 9.7$, $U_\infty = 8700$ fps, Equivalent Altitude = 50 miles

M_∞	Symbol	Reference	Probe Design
≈1.2-2.0	———	Enkenhus (32)	10 deg external chamfer
≈1.7-3.4	——	Sherman (30)	Source shaped, $d_a/D = 0.10$ (These data shown to illustrate effect of nose shape.)
≈9.7	•	LDH Tunnel	Flat-faced, $d_a/D = 0.70$

Note: Enkenhus' results for internally chamfered probe agreed with Sherman's internally chamfered design, and both gave results near curve shown for externally chamfered probe.

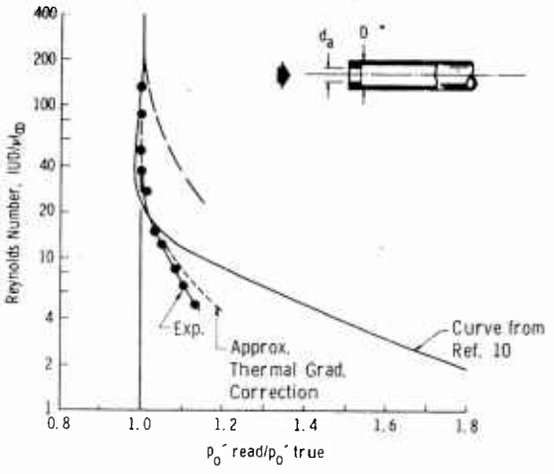

Fig. 18 Viscosity Effect on Readings of Impact-Pressure Probes at Low Reynolds Numbers and Supersonic Speeds

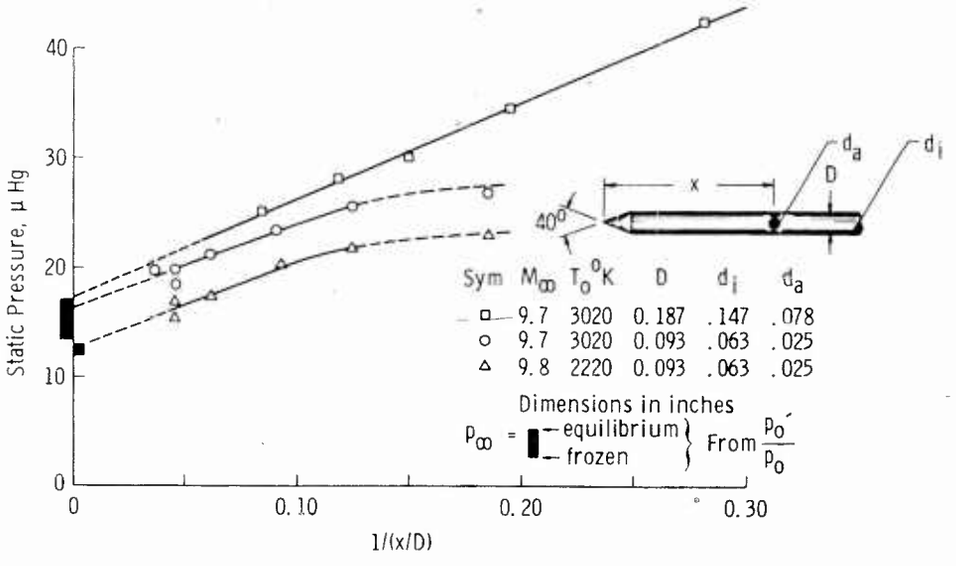

Fig. 19 Approximate Determination of Static Pressure (Data have been corrected for temperature gradient along the probe following Ref. 29.)

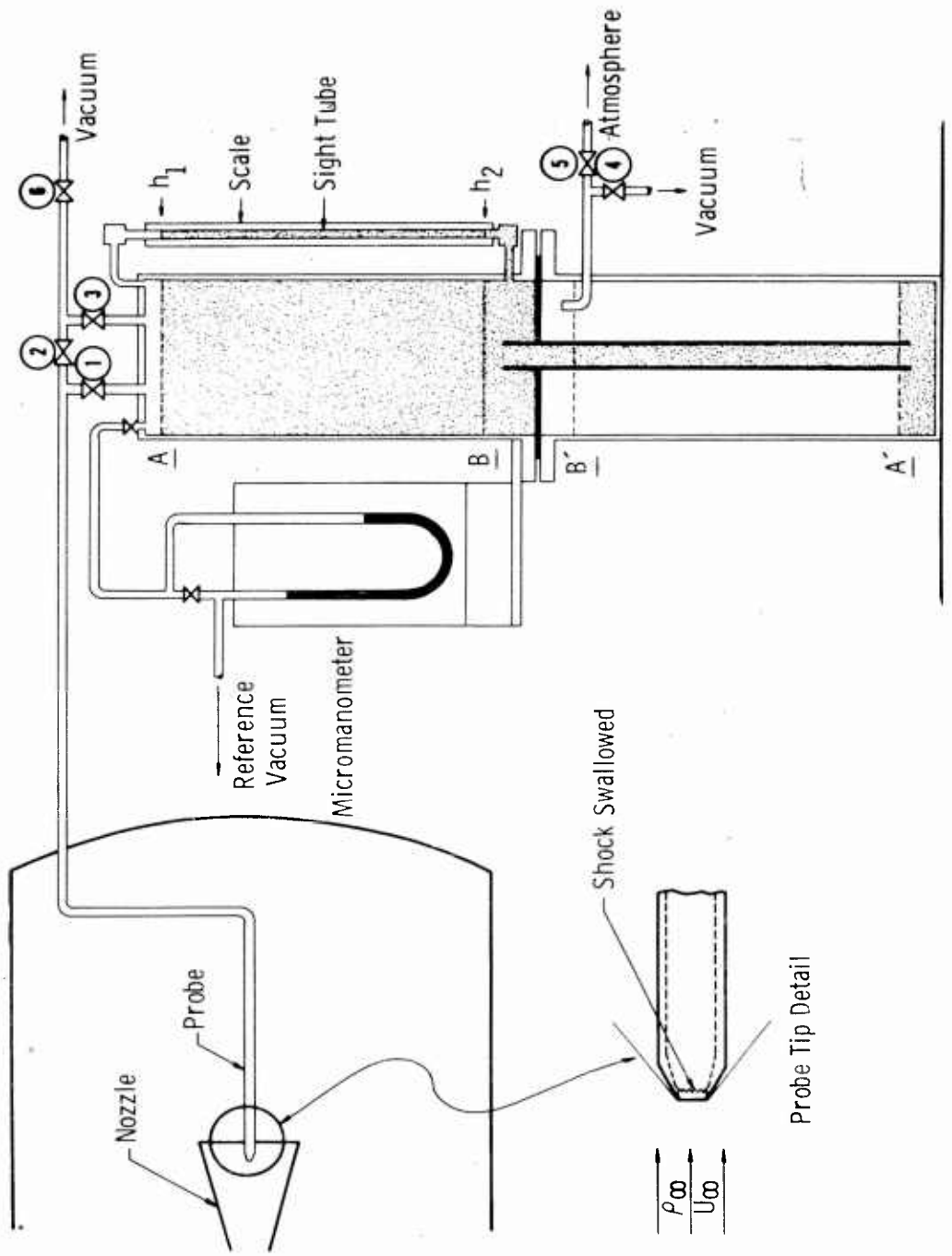

Fig. 20 Schematic Diagram of Mass-Flow Probe System

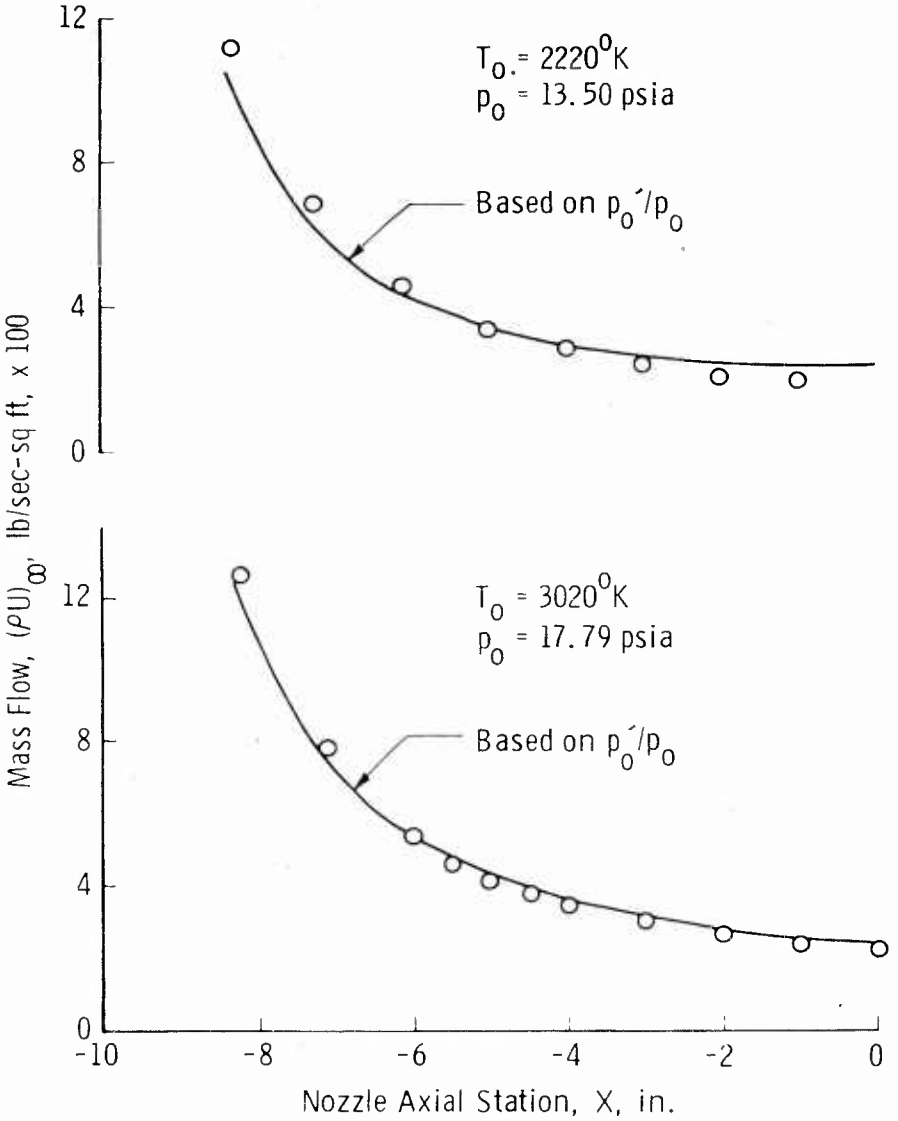

Fig. 21 Measurements with a Mass-Flow Probe (Points represent local values on nozzle C_L.)

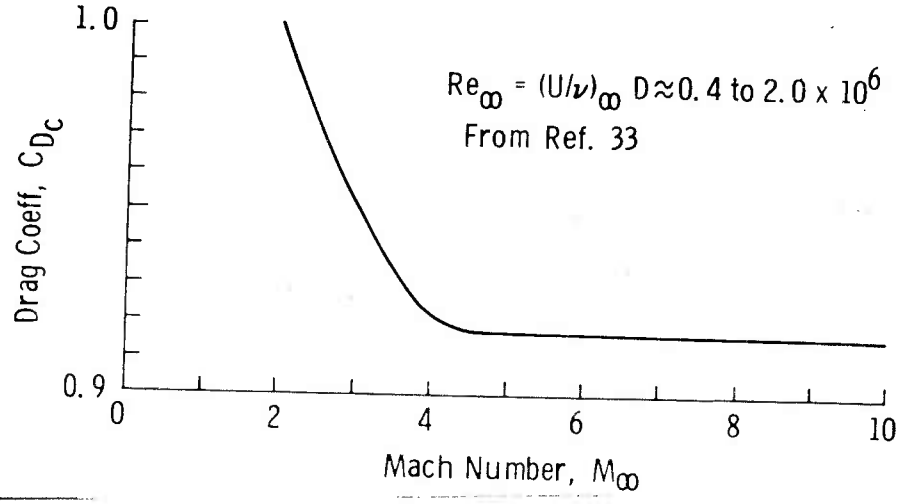

Fig. 22 Drag of Spheres at High Reynolds and Mach Numbers

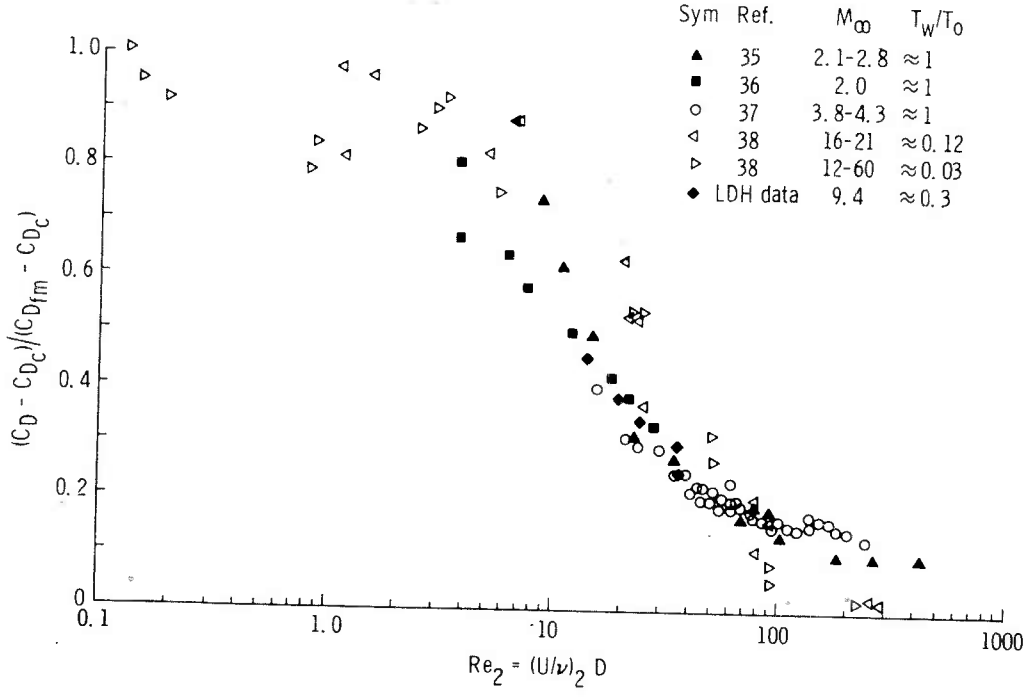

Fig. 23 Comparison of Drag Coefficients of Spheres Measured in Low-Density Wind Tunnels

Cut on broken line

AEDC-TN-61-83

Arnold Engineering Development Center, ARO, Inc., Arnold Air Force Station, Tennessee
DESCRIPTION AND PRELIMINARY CALIBRATION OF A LOW-DENSITY, HYPERVELOCITY WIND TUNNEL by J. Leith Potter, Max Kinslow, George D. Arney, Jr., and Allan B. Bailey, August 1961. 49 pp. (ARO Project Nos. 306060 and 306970) (AFSC Program Area 750A, Project 8950, Task 89602) (AEDC-TN-61-83) (Contract No. AF 40(600)-800 S/A 24(61-73)). Unclassified

38 references

A small, low-density, hypervelocity, continuous wind tunnel operating at total temperatures from 2000 to 4000°K is described, and initial experiments designed to determine the characteristics of the flow are discussed. Effects of low Reynolds numbers on impact-pressure probes and static-pressure probes are shown. Preliminary work with a probe for measuring local mass-flow rate is outlined, and results are shown to be in agreement with impact and static
(over)

UNCLASSIFIED

1. Hypervelocity wind tunnels--Calibration
2. Hypervelocity wind tunnels--Design
3. Low density wind tunnels
4. Pressure--Measurement
5. Spheres--Drag
I. Potter, J. Leith
II. Kinslow, Max
III. Arney, George D., Jr.
IV. Bailey, Allan B.

UNCLASSIFIED

AEDC-TN-61-83

Arnold Engineering Development Center, ARO, Inc., Arnold Air Force Station, Tennessee
DESCRIPTION AND PRELIMINARY CALIBRATION OF A LOW-DENSITY, HYPERVELOCITY WIND TUNNEL by J. Leith Potter, Max Kinslow, George D. Arney, Jr., and Allan B. Bailey, August 1961. 49 pp. (ARO Project Nos. 306060 and 306970) (AFSC Program Area 750A, Project 8950, Task 89602) (AEDC-TN-61-83) (Contract No. AF 40(600)-800 S/A 24(61-73)). Unclassified

38 references

A small, low-density, hypervelocity, continuous wind tunnel operating at total temperatures from 2000 to 4000°K is described, and initial experiments designed to determine the characteristics of the flow are discussed. Effects of low Reynolds numbers on impact-pressure probes and static-pressure probes are shown. Preliminary work with a probe for measuring local mass-flow rate is outlined, and results are shown to be in agreement with impact and static
(over)

UNCLASSIFIED

1. Hypervelocity wind tunnels--Calibration
2. Hypervelocity wind tunnels--Design
3. Low density wind tunnels
4. Pressure--Measurement
5. Spheres--Drag
I. Potter, J. Leith
II. Kinslow, Max
III. Arney, George D., Jr.
IV. Bailey, Allan B.

UNCLASSIFIED

AEDC-TN-61-83

Arnold Engineering Development Center, ARO, Inc., Arnold Air Force Station, Tennessee
DESCRIPTION AND PRELIMINARY CALIBRATION OF A LOW-DENSITY, HYPERVELOCITY WIND TUNNEL by J. Leith Potter, Max Kinslow, George D. Arney, Jr., and Allan B. Bailey, August 1961. 49 pp. (ARO Project Nos. 306060 and 306970) (AFSC Program Area 750A, Project 8950, Task 89602) (AEDC-TN-61-83) (Contract No. AF 40(600)-800 S/A 24(61-73)). Unclassified

38 references

A small, low-density, hypervelocity, continuous wind tunnel operating at total temperatures from 2000 to 4000°K is described, and initial experiments designed to determine the characteristics of the flow are discussed. Effects of low Reynolds numbers on impact-pressure probes and static-pressure probes are shown. Preliminary work with a probe for measuring local mass-flow rate is outlined, and results are shown to be in agreement with impact and static
(over)

UNCLASSIFIED

1. Hypervelocity wind tunnels--Calibration
2. Hypervelocity wind tunnels--Design
3. Low density wind tunnels
4. Pressure--Measurement
5. Spheres--Drag
I. Potter, J. Leith
II. Kinslow, Max
III. Arney, George D., Jr.
IV. Bailey, Allan B.

UNCLASSIFIED

AEDC-TN-61-83

Arnold Engineering Development Center, ARO, Inc., Arnold Air Force Station, Tennessee
DESCRIPTION AND PRELIMINARY CALIBRATION OF A LOW-DENSITY, HYPERVELOCITY WIND TUNNEL by J. Leith Potter, Max Kinslow, George D. Arney, Jr., and Allan B. Bailey, August 1961. 49 pp. (ARO Project Nos. 306060 and 306970) (AFSC Program Area 750A, Project 8950, Task 89602) (AEDC-TN-61-83) (Contract No. AF 40(600)-800 S/A 24(61-73)). Unclassified

38 references

A small, low-density, hypervelocity, continuous wind tunnel operating at total temperatures from 2000 to 4000°K is described, and initial experiments designed to determine the characteristics of the flow are discussed. Effects of low Reynolds numbers on impact-pressure probes and static-pressure probes are shown. Preliminary work with a probe for measuring local mass-flow rate is outlined, and results are shown to be in agreement with impact and static
(over)

UNCLASSIFIED

1. Hypervelocity wind tunnels--Calibration
2. Hypervelocity wind tunnels--Design
3. Low density wind tunnels
4. Pressure--Measurement
5. Spheres--Drag
I. Potter, J. Leith
II. Kinslow, Max
III. Arney, George D., Jr.
IV. Bailey, Allan B.

UNCLASSIFIED

AEDC-TN-61-83

UNCLASSIFIED

pressure measurements. Axial and transverse surveys of flow in the nozzle are presented to illustrate the extent of boundary-layer growth and the useable core of flow. A diffuser is proved to be advantageous, even though very low Reynolds numbers are typical of the tunnel. A comparison of data on drag of spheres, including measurements from the new wind tunnel, is presented.

UNCLASSIFIED

AEDC-TN-61-83

UNCLASSIFIED

pressure measurements. Axial and transverse surveys of flow in the nozzle are presented to illustrate the extent of boundary-layer growth and the useable core of flow. A diffuser is proved to be advantageous, even though very low Reynolds numbers are typical of the tunnel. A comparison of data on drag of spheres, including measurements from the new wind tunnel, is presented.

UNCLASSIFIED

AEDC-TN-61-83

UNCLASSIFIED

pressure measurements. Axial and transverse surveys of flow in the nozzle are presented to illustrate the extent of boundary-layer growth and the useable core of flow. A diffuser is proved to be advantageous, even though very low Reynolds numbers are typical of the tunnel. A comparison of data on drag of spheres, including measurements from the new wind tunnel, is presented.

UNCLASSIFIED

AEDC-TN-61-83

UNCLASSIFIED

pressure measurements. Axial and transverse surveys of flow in the nozzle are presented to illustrate the extent of boundary-layer growth and the useable core of flow. A diffuser is proved to be advantageous, even though very low Reynolds numbers are typical of the tunnel. A comparison of data on drag of spheres, including measurements from the new wind tunnel, is presented.

UNCLASSIFIED

Cut on broken line

AEDC-TN-61-83

Arnold Engineering Development Center, ARO, Inc., Arnold Air Force Station, Tennessee
DESCRIPTION AND PRELIMINARY CALIBRATION OF A LOW-DENSITY, HYPERVELOCITY WIND TUNNEL by J. Leith Potter, Max Kinslow, George D. Arney, Jr., and Allan B. Bailey, August 1961. 49 pp. (ARO Project Nos. 306060 and 306970) (AFSC Program Area 750A, Project 8950, Task 89602) (AEDC-TN-61-83) (Contract No. AF 40(600)-800 S/A 24(61-73)). Unclassified

38 references

A small, low-density, hypervelocity, continuous wind tunnel operating at total temperatures from 2000 to 4000°K is described, and initial experiments designed to determine the characteristics of the flow are discussed. Effects of low Reynolds numbers on impact-pressure probes and static-pressure probes are shown. Preliminary work with a probe for measuring local mass-flow rate is outlined, and results are shown to be in agreement with impact and static (over)

UNCLASSIFIED

1. Hypervelocity wind tunnels--Calibration
2. Hypervelocity wind tunnels--Design
3. Low density wind tunnels
4. Pressure--Measurement
5. Spheres--Drag

I. Potter, J. Leith
II. Kinslow, Max
III. Arney, George D., Jr.
IV. Bailey, Allan B.

UNCLASSIFIED

AEDC-TN-61-83

Arnold Engineering Development Center, ARO, Inc., Arnold Air Force Station, Tennessee
DESCRIPTION AND PRELIMINARY CALIBRATION OF A LOW-DENSITY, HYPERVELOCITY WIND TUNNEL by J. Leith Potter, Max Kinslow, George D. Arney, Jr., and Allan B. Bailey, August 1961. 49 pp. (ARO Project Nos. 306060 and 306970) (AFSC Program Area 750A, Project 8950, Task 89602) (AEDC-TN-61-83) (Contract No. AF 40(600)-800 S/A 24(61-73)). Unclassified

38 references

A small, low-density, hypervelocity, continuous wind tunnel operating at total temperatures from 2000 to 4000°K is described, and initial experiments designed to determine the characteristics of the flow are discussed. Effects of low Reynolds numbers on impact-pressure probes and static-pressure probes are shown. Preliminary work with a probe for measuring local mass-flow rate is outlined, and results are shown to be in agreement with impact and static (over)

UNCLASSIFIED

1. Hypervelocity wind tunnels-Calibration
2. Hypervelocity wind tunnels-Design
3. Low density wind tunnels
4. Pressure--Measurement
5. Spheres--Drag

I. Potter, J. Leith
II. Kinslow, Max
III. Arney, George D., Jr.
IV. Bailey, Allan B.

UNCLASSIFIED

AEDC-TN-61-83

Arnold Engineering Development Center, ARO, Inc., Arnold Air Force Station, Tennessee
DESCRIPTION AND PRELIMINARY CALIBRATION OF A LOW-DENSITY, HYPERVELOCITY WIND TUNNEL by J. Leith Potter, Max Kinslow, George D. Arney, Jr., and Allan B. Bailey, August 1961. 49 pp. (ARO Project Nos. 306060 and 306970) (AFSC Program Area 750A, Project 8950, Task 89602) (AEDC-TN-61-83) (Contract No. AF 40(600)-800 S/A 24(61-73)). Unclassified

38 references

A small, low-density, hypervelocity, continuous wind tunnel operating at total temperatures from 2000 to 4000°K is described, and initial experiments designed to determine the characteristics of the flow are discussed. Effects of low Reynolds numbers on impact-pressure probes and static-pressure probes are shown. Preliminary work with a probe for measuring local mass-flow rate is outlined, and results are shown to be in agreement with impact and static (over)

UNCLASSIFIED

1. Hypervelocity wind tunnels--Calibration
2. Hypervelocity wind tunnels--Design
3. Low density wind tunnels
4. Pressure--Measurement
5. Spheres--Drag

I. Potter, J. Leith
II. Kinslow, Max
III. Arney, George D., Jr.
IV. Bailey, Allan B.

UNCLASSIFIED

AEDC-TN-61-83

Arnold Engineering Development Center, ARO, Inc., Arnold Air Force Station, Tennessee
DESCRIPTION AND PRELIMINARY CALIBRATION OF A LOW-DENSITY, HYPERVELOCITY WIND TUNNEL by J. Leith Potter, Max Kinslow, George D. Arney, Jr., and Allan B. Bailey, August 1961. 49 pp. (ARO Project Nos. 306060 and 306970) (AFSC Program Area 750A, Project 8950, Task 89602) (AEDC-TN-61-83) (Contract No. AF 40(600)-800 S/A 24(61-73)). Unclassified

38 references

A small, low-density, hypervelocity, continuous wind tunnel operating at total temperatures from 2000 to 4000°K is described, and initial experiments designed to determine the characteristics of the flow are discussed. Effects of low Reynolds numbers on impact-pressure probes and static-pressure probes are shown. Preliminary work with a probe for measuring local mass-flow rate is outlined, and results are shown to be in agreement with impact and static (over)

UNCLASSIFIED

1. Hypervelocity wind tunnels-Calibration
2. Hypervelocity wind tunnels-Design
3. Low density wind tunnels
4. Pressure--Measurement
5. Spheres--Drag

I. Potter, J. Leith
II. Kinslow, Max
III. Arney, George D., Jr.
IV. Bailey, Allan B.

UNCLASSIFIED

AEDC-TN-61-83

UNCLASSIFIED

pressure measurements. Axial and transverse surveys of flow in the nozzle are presented to illustrate the extent of boundary-layer growth and the useable core of flow. A diffuser is proved to be advantageous, even though very low Reynolds numbers are typical of the tunnel. A comparison of data on drag of spheres, including measurements from the new wind tunnel, is presented.

UNCLASSIFIED

AEDC-TN-61-83

UNCLASSIFIED

pressure measurements. Axial and transverse surveys of flow in the nozzle are presented to illustrate the extent of boundary-layer growth and the useable core of flow. A diffuser is proved to be advantageous, even though very low Reynolds numbers are typical of the tunnel. A comparison of data on drag of spheres, including measurements from the new wind tunnel, is presented.

UNCLASSIFIED

AEDC-TN-61-83

UNCLASSIFIED

pressure measurements. Axial and transverse surveys of flow in the nozzle are presented to illustrate the extent of boundary-layer growth and the useable core of flow. A diffuser is proved to be advantageous, even though very low Reynolds numbers are typical of the tunnel. A comparison of data on drag of spheres, including measurements from the new wind tunnel, is presented.

UNCLASSIFIED

AEDC-TN-61-83

UNCLASSIFIED

pressure measurements. Axial and transverse surveys of flow in the nozzle are presented to illustrate the extent of boundary-layer growth and the useable core of flow. A diffuser is proved to be advantageous, even though very low Reynolds numbers are typical of the tunnel. A comparison of data on drag of spheres, including measurements from the new wind tunnel, is presented.

UNCLASSIFIED

Cut on broken line

AEDC-TN-61-83

Arnold Engineering Development Center, ARO, Inc., Arnold Air Force Station, Tennessee
DESCRIPTION AND PRELIMINARY CALIBRATION OF A LOW-DENSITY, HYPERVELOCITY WIND TUNNEL by J. Leith Potter, Max Kinslow, George D. Arney, Jr., and Allan B. Bailey, August 1961. 49 pp. (ARO Project Nos. 306060 and 306970) (AFSC Program Area 750A, Project 8950, Task 89602) (AEDC-TN-61-83) (Contract No. AF 40(600)-800 S/A 24(61-73)). Unclassified

38 references

A small, low-density, hypervelocity, continuous wind tunnel operating at total temperatures from 2000 to 4000°K is described, and initial experiments designed to determine the characteristics of the flow are discussed. Effects of low Reynolds numbers on impact-pressure probes and static-pressure probes are shown. Preliminary work with a probe for measuring local mass-flow rate is outlined, and results are shown to be in agreement with impact and static
(over)

UNCLASSIFIED

1. Hypervelocity wind tunnels--Calibration
2. Hypervelocity wind tunnels--Design
3. Low density wind tunnels
4. Pressure--Measurement
5. Spheres--Drag
I. Potter, J. Leith
II. Kinslow, Max
III. Arney, George D., Jr.
IV. Bailey, Allan B.

UNCLASSIFIED

AEDC-TN-61-83

Arnold Engineering Development Center, ARO, Inc., Arnold Air Force Station, Tennessee
DESCRIPTION AND PRELIMINARY CALIBRATION OF A LOW-DENSITY, HYPERVELOCITY WIND TUNNEL by J. Leith Potter, Max Kinslow, George D. Arney, Jr., and Allan B. Bailey, August 1961. 49 pp. (ARO Project Nos. 306060 and 306970) (AFSC Program Area 750A, Project 8950, Task 89602) (AEDC-TN-61-83) (Contract No. AF 40(600)-800 S/A 24(61-73)). Unclassified

38 references

A small, low-density, hypervelocity, continuous wind tunnel operating at total temperatures from 2000 to 4000°K is described, and initial experiments designed to determine the characteristics of the flow are discussed. Effects of low Reynolds numbers on impact-pressure probes and static-pressure probes are shown. Preliminary work with a probe for measuring local mass-flow rate is outlined, and results are shown to be in agreement with impact and static
(over)

UNCLASSIFIED

1. Hypervelocity wind tunnels--Calibration
2. Hypervelocity wind tunnels--Design
3. Low density wind tunnels
4. Pressure--Measurement
5. Spheres--Drag
I. Potter, J. Leith
II. Kinslow, Max
III. Arney, George D., Jr.
IV. Bailey, Allan B.

UNCLASSIFIED

AEDC-TN-61-83

Arnold Engineering Development Center, ARO, Inc., Arnold Air Force Station, Tennessee
DESCRIPTION AND PRELIMINARY CALIBRATION OF A LOW-DENSITY, HYPERVELOCITY WIND TUNNEL by J. Leith Potter, Max Kinslow, George D. Arney, Jr., and Allan B. Bailey, August 1961. 49 pp. (ARO Project Nos. 306060 and 306970) (AFSC Program Area 750A, Project 8950, Task 89602) (AEDC-TN-61-83) (Contract No. AF 40(600)-800 S/A 24(61-73)). Unclassified

38 references

A small, low-density, hypervelocity, continuous wind tunnel operating at total temperatures from 2000 to 4000°K is described, and initial experiments designed to determine the characteristics of the flow are discussed. Effects of low Reynolds numbers on impact-pressure probes and static-pressure probes are shown. Preliminary work with a probe for measuring local mass-flow rate is outlined, and results are shown to be in agreement with impact and static
(over)

UNCLASSIFIED

1. Hypervelocity wind tunnels--Calibration
2. Hypervelocity wind tunnels--Design
3. Low density wind tunnels
4. Pressure--Measurement
5. Spheres--Drag
I. Potter, J. Leith
II. Kinslow, Max
III. Arney, George D., Jr.
IV. Bailey, Allan B.

UNCLASSIFIED

AEDC-TN-61-83

Arnold Engineering Development Center, ARO, Inc., Arnold Air Force Station, Tennessee
DESCRIPTION AND PRELIMINARY CALIBRATION OF A LOW-DENSITY, HYPERVELOCITY WIND TUNNEL by J. Leith Potter, Max Kinslow, George D. Arney, Jr., and Allan B. Bailey, August 1961. 49 pp. (ARO Project Nos. 306060 and 306970) (AFSC Program Area 750A, Project 8950, Task 89602) (AEDC-TN-61-83) (Contract No. AF 40(600)-800 S/A 24(61-73)). Unclassified

38 references

A small, low-density, hypervelocity, continuous wind tunnel operating at total temperatures from 2000 to 4000°K is described, and initial experiments designed to determine the characteristics of the flow are discussed. Effects of low Reynolds numbers on impact-pressure probes and static-pressure probes are shown. Preliminary work with a probe for measuring local mass-flow rate is outlined, and results are shown to be in agreement with impact and static
(over)

UNCLASSIFIED

1. Hypervelocity wind tunnels--Calibration
2. Hypervelocity wind tunnels--Design
3. Low density wind tunnels
4. Pressure--Measurement
5. Spheres--Drag
I. Potter, J. Leith
II. Kinslow, Max
III. Arney, George D., Jr.
IV. Bailey, Allan B.

UNCLASSIFIED

AEDC-TN-61-83

pressure measurements. Axial and transverse surveys of flow in the nozzle are presented to illustrate the extent of boundary-layer growth and the useable core of flow. A diffuser is proved to be advantageous, even though very low Reynolds numbers are typical of the tunnel. A comparison of data on drag of spheres, including measurements from the new wind tunnel, is presented.

UNCLASSIFIED

UNCLASSIFIED

AEDC-TN-61-83

pressure measurements. Axial and transverse surveys of flow in the nozzle are presented to illustrate the extent of boundary-layer growth and the useable core of flow. A diffuser is proved to be advantageous, even though very low Reynolds numbers are typical of the tunnel. A comparison of data on drag of spheres, including measurements from the new wind tunnel, is presented.

UNCLASSIFIED

UNCLASSIFIED

AEDC-TN-61-83

pressure measurements. Axial and transverse surveys of flow in the nozzle are presented to illustrate the extent of boundary-layer growth and the useable core of flow. A diffuser is proved to be advantageous, even though very low Reynolds numbers are typical of the tunnel. A comparison of data on drag of spheres, including measurements from the new wind tunnel, is presented.

UNCLASSIFIED

UNCLASSIFIED

AEDC-TN-61-83

pressure measurements. Axial and transverse surveys of flow in the nozzle are presented to illustrate the extent of boundary-layer growth and the useable core of flow. A diffuser is proved to be advantageous, even though very low Reynolds numbers are typical of the tunnel. A comparison of data on drag of spheres, including measurements from the new wind tunnel, is presented.

UNCLASSIFIED

UNCLASSIFIED

UNCLASSIFIED